INSTITUT DE FRANCE
Académie des sciences

Comptes Rendus
Géoscience
Sciences de la Planète

José Emilio Cortés

Dating volcanic materials through biochronostratigraphic methods applied to hosting strata (example from the Iberian Chain, eastern Spain)

Volume 355 (2023), p. 175-201

Published online: 12 June 2023

https://doi.org/10.5802/crgeos.220

CENTRE MERSENNE

Les Comptes Rendus. Géoscience — Sciences de la Planète *sont membres du Centre Mersenne pour l'édition scientifique ouverte*
www.centre-mersenne.org
e-ISSN : 1778-7025

Comptes Rendus
Géoscience — Sciences de la Planète
2023, Vol. 355, p. 175-201
https://doi.org/10.5802/crgeos.220

Research article — Volcanology

Dating volcanic materials through biochronostratigraphic methods applied to hosting strata (example from the Iberian Chain, eastern Spain)

José Emilio Cortés [a]

[a] Departamento de Geodinámica, Estratigrafía y Paleontología, Facultad de Ciencias Geológicas, Universidad Complutense de Madrid, José Antonio Novais 12, 28040 Madrid, Spain

E-mail: jocortes@ucm.es

Abstract. Volcaniclastic accumulations in shallow marine environments are prone to be eroded and transported by sedimentary agents and then resedimented either on contemporaneous or younger substrates. Therefore, dating of the volcanic events through the sediments containing interbedded volcanic layers can lead to errors. A case study of volcanism in the southeastern Iberian Range during the Early and Middle Jurassic is presented. Precise dating of hosting carbonate sediments based on ammonite and brachiopod biochronostratigraphic method has allowed distinguishing 13 volcanic levels of different ages ranging from the early Pliensbachian to the early Bajocian. A set of petrological, geomorphological, sedimentological, and paleontological criteria are applied in order to discriminate primary from secondary (epiclastic) volcaniclastic deposits and thus make it possible to match the ages of primary volcaniclastic deposits with volcanic eruptions. Implementation of such criteria has confirmed that the early Pliensbachian–early Bajocian interval (ca. 20 Ma) corresponds with the actual period of volcanic activity.

Keywords. Jurassic magmatism, Iberian range, Volcanism dating, Biostratigraphic age, Intraplate volcanism.

Manuscript received 13 March 2022, revised 7 July 2022 and 9 November 2022, accepted 12 May 2023.

1. Introduction

Volcanic activity recorded over time is often displayed in ancient marine environments as multi-episodic volcanogenic deposits interbedded within sediments. Dating these volcanic manifestations and ascertaining the genuine age of the volcanism are essential steps with a direct impact on understanding the geodynamic context of the sedimentary basin, as well as a significant starting point for many different studies (e.g., magnetostratigraphic ones, including the refinement of the Geomagnetic Polarity Time Scale for periods preceding the present-day oceanic magnetic record).

In this work, a case study of a shallow-marine and exceptionally ammonite- and brachiopod-rich Lower–Middle Jurassic carbonate succession of the Iberian Range (Spain) is presented. They were deposited along the Iberian shelf during the opening of the westernmost Tethys Ocean. These carbonate sediments include a series of volcanic levels mostly made of explosive pyroclastic to epiclastic deposits and rare lava flows, whose mineral composition shows alkaline affinity compatible with an extensional regime [e.g., Gautier, 1968, Ortí and Sanfeliu, 1971, Gómez, 1979, Ortí and Vaquer, 1980, Ortí, 1987, Ancochea et al., 1988, Lago et al., 1996, 2004, Martínez et al., 1996a,c,d, 1997a, 1998, Valenzuela et al., 1996, Cortés, 2018].

The marine strata containing the interbedded volcanic levels display a high fossil content (particularly ammonites and brachiopods) with possibilities of providing accurate biostratigraphic ages. This is possible because of the rapid evolution over time of ammonoids, allowing near-global precise standard zonations [e.g., Torrens, 2002, Page, 2003, Callomon, 2003].

This scenario would be the reverse situation of the "interbedded volcanic rocks (PLAN A)" of Copeland [2020], in which fossiliferous-rich sedimentary strata are located above and below the volcanic deposit pending dating. The situation for consideration here likewise matches the "biostratigraphy (PLAN B)" of Copeland [2020], yet replacing the sandstone bed with a volcanic body of interest to be dated.

Furthermore, this work aims to verify whether the interbedded volcanic levels correlate with volcanic events by using a set of criteria to identify primary volcanic deposits in the Lower and Middle Jurassic sedimentary series from the Iberian Chain.

2. Geological setting

2.1. *Paleogeographic and geodynamic context*

The Pangea supercontinent began to break up in the late Permian, initiating the Alpine Cycle, throughout a series of rifting areas developed with preference along weakness zones such as old suture lineaments between ancient tectonic plates [Quesada and Oliveira, 2019]. It continued opening in Jurassic time resulting in two major (Atlantic and Tethyan) tectonic domains. Precise paleogeography of continents and oceans in the western Tethys during the Jurassic is controversial and remains under discussion. The different existing paleogeographic-reconstruction models still demonstrate a certain amount of disagreements, for instance, in the number of oceanic domains (e.g., Ligurian or Alpine Tethys, Betic ocean, Magrhebian Tethys) or the position of fragmented microplates [Poulaki and Stockli, 2022, and references therein]. Nevertheless, a consensus about many additional issues has been reached. Thus, about Late Triassic–Early Jurassic times, the Paleotethys had been virtually closed and consumed in favor of the Neotethys Ocean opened to the south. Many terranes (e.g., Cimmerian) drifted northward and then attached to the Euroasian Plate as a result of this Paleotethys Ocean subduction [Schettino and Turco, 2011]. The westernmost extension of the Neotethys was the SW–NE trending Alpine Tethys Ocean. This spreading rifted structure constituted a magma-poor rift system [Manatschal et al., 2021] which began to develop during the Early Jurassic [Schettino and Turco, 2011].

Iberia, located between the African, Eurasian, and North American plates, played a significant role in shaping plate boundaries in the western Neotethys and Atlantic realms (Figure 1). The western margin of Iberia was constituted by a series of rift basins developed along the future axis of the North Atlantic Ocean [Berra and Angiolini, 2014]. The southwestmost segment (Ligurian) of the Alpine Tethys represented the southeast Iberian boundary [Schettino and Turco, 2011, Manatschal et al., 2021]. Two transfer zones had fundamental implications for the Iberia-Europe and the Iberia-Africa boundaries: Gibraltar and the North Pyrenean transfer zones [Schettino and Turco, 2011, Angrand and Mouthereau, 2021]. The Central Atlantic jointed with the westward propagating Ligurian-Alpine mid-ocean ridge around the Pliensbachian [Puga et al., 2011, Schettino and Turco, 2011] through the Gibraltar transfer zone. At the Tithonian time, the kinematics of the Gibraltar transfer zone jumped northward to the North Pyrenean transfer zone [Schettino and Turco, 2011].

The western half of Iberia was occupied by the emerged Iberian Massif. Its eastern half was constituted by a set of intracratonic basins developed at the same time as the Permo–Triassic rift systems, at the beginning of the Pangea break up, partly reactivating structures inherited from the Variscan orogeny [Osete et al., 2011, Vergés et al., 2019]. In this scenario, the Iberian basin was a carbonate-platform system that constituted the proximal part of the

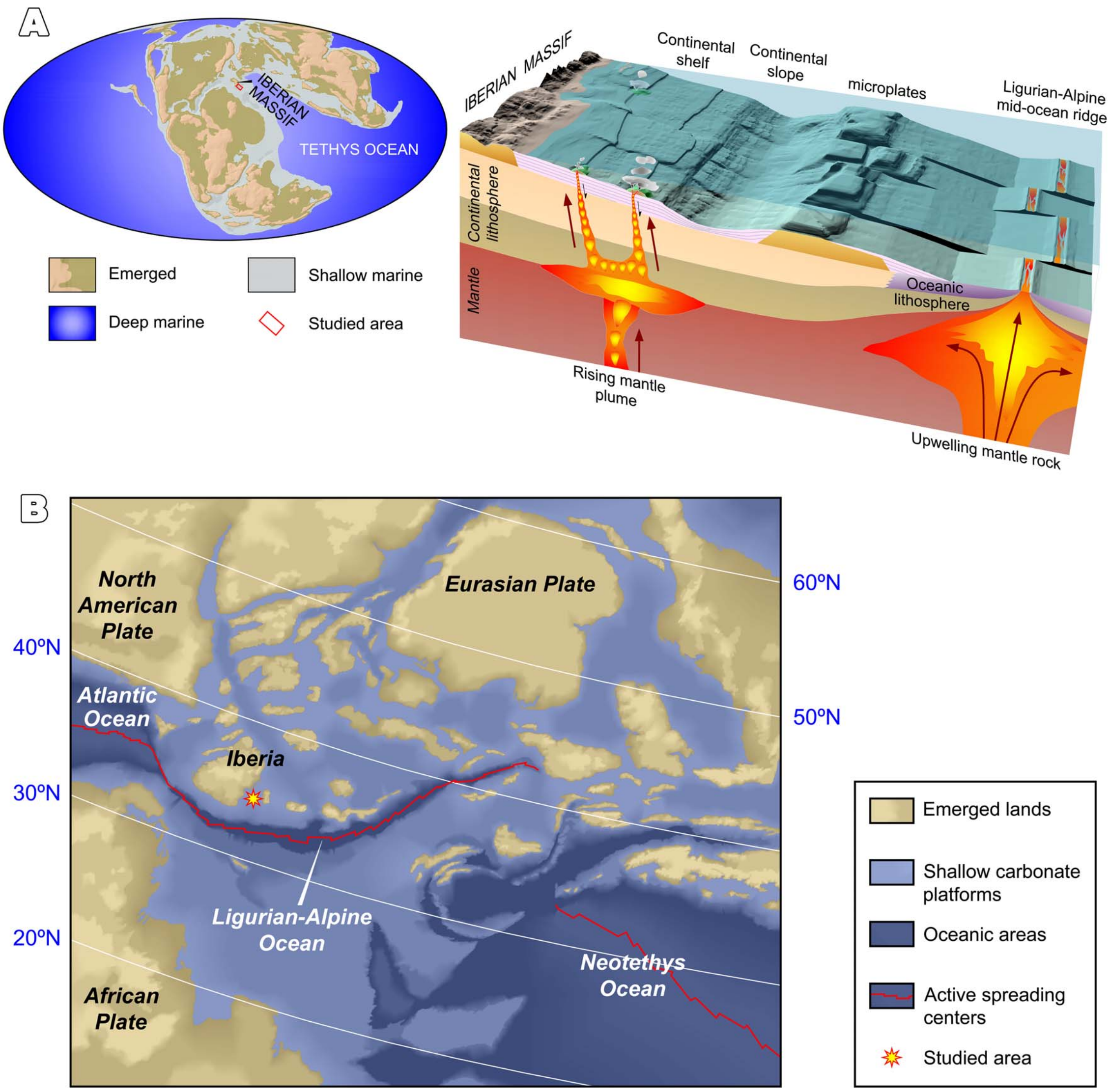

Figure 1. (A) 3D reconstruction of the eastern edge of the Iberian Massif, continental shelf and slope, microplates located between Iberia and the Alpine oceanic crust [according to the kinematic reconstructions by Schettino and Turco, 2011], Ligurian-Alpine mid-ocean ridge, and magmatic plumbing system. (B) Paleogeographic reconstruction of the western Tethys during the Early–Middle Jurassic [modified from Schettino and Turco, 2011 and Blakey, 2011. Paleolatitudes adapted from Osete et al., 2011].

eastern paleomargin of Iberia [Gómez et al., 2004] and recorded alkaline basaltic eruptions interbedded within shallow-marine sediments at 30–35° N latitude [according to Osete et al., 2011] (Figure 1).

The time interval (early Pliensbachian–early Bajocian) in which the studied volcanic deposits were accumulated fits within the first passive margin or post-rifting stage in the Iberian Basin, from the latest Triassic (late Norian) [Sánchez-Moya and Sopeña, 2004, Gómez et al., 2019] or Early Jurassic (Sinemurian) [Salas and Casas, 1993, Salas et al., 2001] to Middle–Late Jurassic (Callovian–Oxfordian boundary) [Gómez et al., 2019] or latest Oxfordian [Salas and Casas, 1993, Salas et al., 2001, Sánchez-Moya and

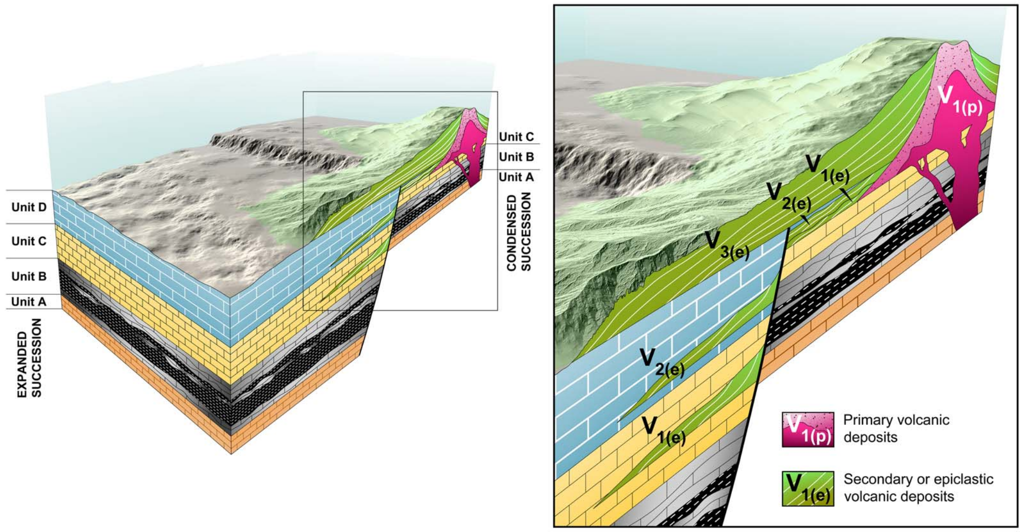

Figure 2. Idealized landscape showing the interaction between submarine volcanism, tectonism, and sedimentation. A volcanic cone formed over an upthrown block with low rates of subsidence. As a consequence, the volcanic cone undergoes dismantling. Parts of the volcanic material are intermittently eroded, transported, and redeposited in the downthrown block, with higher subsidence rates. Several epiclastic (secondary volcaniclastic) bodies were interbedded in the sedimentary succession. $V_{1(e)}$ was redeposited upon a substrate coeval with the substrate on which lies the primary volcanic cone $V_{1(p)}$. So, the age of its stratigraphic emplacement matches the age of the primary volcanic cone and, therefore, matches the timing of volcanism. $V_{2(e)}$ and $V_{3(e)}$ were redeposited upon younger substrates than that substrate on which the volcanic cone lies. Therefore, the stratigraphic ages of $V_{2(e)}$ and $V_{3(e)}$ differ from the age of the stratigraphic emplacement of the volcanic cone. Again, these do not concur with the timing of the volcanism.

Sopeña, 2004]. Most of the total volcanic materials were accumulated in shallow to very shallow marine environments. The volcanic activity in shallow submarine settings tends to be explosive due to the contact between the ambient seawater and the magma and also because the hydrostatic pressure is generally negligible [Cas and Wright, 1987, Cas, 1992, White et al., 2003, Cas and Giordano, 2014]. A part or whole of the volcanic bodies might likely have been redeposited on substrates younger than those in which they were initially deposited (Figure 2).

The Cretaceous and Cenozoic shortening occurred during the subsequent Alpine orogenic stage and gave rise to the Alpine ranges (the Basque-Cantabrian, Pyrenean, Catalonian, Iberian, and Betic ranges). The Iberian Range is a moderately deformed intraplate chain constituted by a NW-oriented folded belt with a low degree of shortening [Gómez et al., 2019]. The Castilian–Valencian Branch and the Aragonese Branch are two NW–SE-oriented elongated areas that form its central and eastern part. The studied area locates at the confluence of both branches (Figure 3A,B,C).

2.2. *Petrography*

Ancochea et al. [1988] examined the volcanic rocks that crop out on the road connecting the towns of La Puebla de Valverde and Camarena de la Sierra and their surroundings. The lava samples studied are made of olivine basalts and subordinate plagioclase-rich basalts. They mostly show porphyritic textures, displaying varying amounts of olivine and clinopyroxene phenocrysts within a fine-grained microlitic groundmass with plagioclase, clinopyroxene, and olivine. Volcanic rocks are intensively altered as shown by silicification and serpentinization. They are derived from alkaline or middle-alkaline magmas

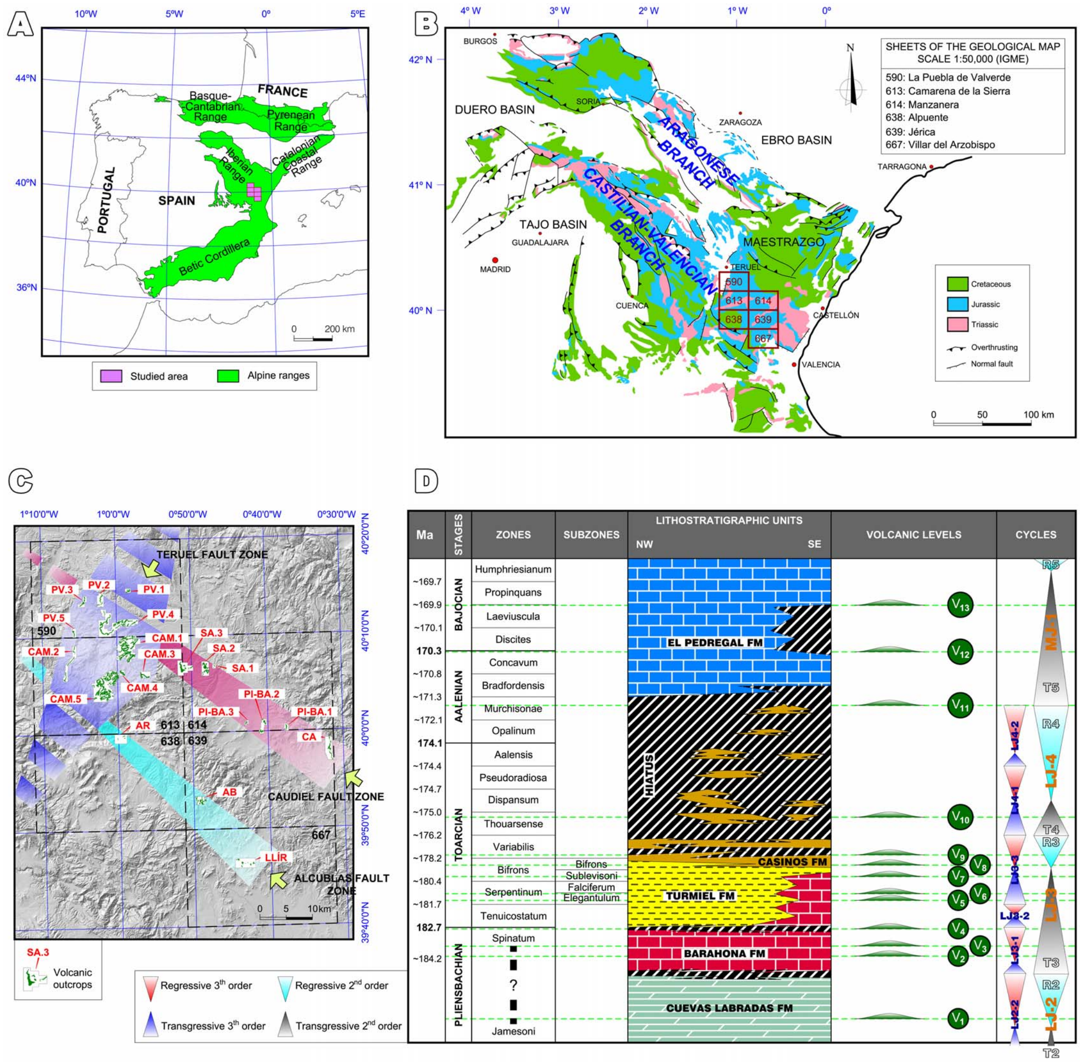

Figure 3. (A) Location of the studied area in the Iberian Range. (B) Geological location of the six sheets of the National Topographic Map at the scale of 1:50,000 in which the studied area is included. (C) Location of volcanic outcrops along the Caudiel, Alcublas, and Teruel fault zones within the studied area. Outcrops abbreviations: CA (Caudiel), PI-BA.1, 2, and 3 (Pina-Barracas.1, 2, and 3), SA.1, 2, and 3 (Sarrión.1, 2, and 3), LLÍR (Llíria), AB (Abejuela), AR (Arcos de las Salinas), PV.1, 2, 3, 4, and 5 (La Puebla de Valverde.1, 2, 3, 4, and 5), CAM.1, 2, 3, 4, and 5 (Camarena de la Sierra.1, 2, 3, 4, and 5). (D) Synthetic chronostratigraphic chart, showing stages, ammonite zones, lithostratigraphic units, volcanic levels, and stratigraphic cycles. Cycles were defined by Gómez and Goy [2000, 2005] and Gómez et al. [2004]. Ammonite zones—and subzones—for the Lower Jurassic are the "Standard Zones" of Page [2003] for the Northwest European Province (Pliensbachian and late Toarcian) and the Submediterranean Province (early Toarcian). The ammonite zonation of the Aalenian and Bajocian stages reproduces the biochronostratigraphic scheme figured by Fernández-López [1985] and Pavia and Fernández-López [2016, 2019] for the Mediterranean–Caucasian Subrealm. Data showing the relative ages of the 13 volcanic levels as revealed in Cortés [2018, 2020, 2021]. Absolute ages for the boundaries of the ammonite zones are obtained from Gradstein et al. [2012]. Absolute ages for the boundaries of the stages have been taken from Cohen et al. [2013].

that could have been generated by a moderate degree of melting of the upper mantle reflecting enrichment of incompatible elements. The melt underwent moderate fractionation (11–16%) of olivine and clinopyroxene phases [Ancochea et al., 1988].

Martínez et al. [1996a,c,d, 1997a,b, 1998] and Martínez-González et al. [1996] also studied lava flows and isolated lava bombs included within a pyroclastic pile in the Javalambre ranges area. They are made of porphyritic basaltic rocks with a microlitic groundmass with plagioclase, olivine, and subordinate clinopyroxene minerals. Phenocrysts are made of olivine and titanaugite with concentric zoning. Hematite, ilmenite, titanomagnetite, and spinel are common subordinate opaque minerals. The mineral association indicates an alkaline affinity, confirmed by the chemical composition of clinopyroxenes [Martínez et al., 1996a,c,d, 1997a,b, 1998, Martínez-González et al., 1996]. Ancochea et al. [1988], Martínez et al. [1996a,c,d, 1997a,b, 1998] and Martínez-González et al. [1996] claimed that the volcanism occurred in intraplate domains, being controlled by the development of fracture systems during an extensional period.

2.3. *Stratigraphic record*

All volcanic bodies are embedded within the Cuevas Labradas (upper part), Barahona, Turmiel, Casinos, and the lower part of the El Pedregal Formations (Figure 3D) [Cortés, 2018]. The Cuevas Labradas Formation is constituted by mudstones, bioclastic wackestones to packstones, cross-bedded grainstones, crystalline dolostones, and bindstones (algal mats). Locally, greenish-yellow marls and calcareous breccias are dominant. Overall, facies associations reflect subtidal, restricted lagoon, low- and high-energy intertidal, and supratidal (salt flat) environments. The age interval ranges from the late Sinemurian to the early Pliensbachian (Davoei Zone) up to the late Pliensbachian (Margaritatus Zone) locally [Goy et al., 1976, Gómez et al., 2004].

The Barahona Formation comprises bioclastic wackestones to packstones with chert nodules and hardgrounds, sometimes grainstones, and occasional marly interbeds. Sedimentation took place in relatively shallow subtidal platforms, usually located below the fair-weather wave base but influenced by storm activity and colonized by benthic organisms (mainly crinoids, oysters, and scarce brachiopods). Nevertheless, beach fronts form where bioclastic shoals emerged, showing tractional structures. The Barahona Formation ranges in age from the late Pliensbachian (Margaritatus Zone p.p.) to the early Toarcian (Tenuicostatum Zone p.p.) [Goy et al., 1976, Gómez et al., 2004].

The Turmiel Formation is composed of alternating marls and mudstones to packstones. They were deposited in low-energy, external, and open marine carbonate platforms generally placed below the storm wave base. Lithology, facies associations and diversity of benthic fauna (echinoids, bivalves, bryozoans, brachiopods) indicate widespread deepening of the Iberian carbonate-platform system. The ammonites are more abundant than in the older, previously described formations, especially matching the maximum peaks of accommodation. The Turmiel Formation is Toarcian in age (Tenuicostatum Zone–Bifrons Zone), but the lower part can be late Pliensbachian (Spinatum Zone), and the upper part can locally reach the early Aalenian (Opalinum Zone) [Goy et al., 1976, Gómez and Goy, 2000, Gómez et al., 2004].

The Casinos Formation is characterized by mudstones, bioclastic wackestones, and local packstones. In the uppermost part, the formation sometimes shows ferruginous or phosphatic oolites and episodes of regional emersion. Thin marly beds often occur in the lower part of the formation. Facies associations and organisms (crinoids, inoceramids, oysters, brachiopods, gastropods, belemnites, and necroplanktic drifted ammonoid shells) are indicators of external, shallow, and open carbonate platform settings. The Casinos Formation extends from the early Toarcian (Bifrons Zone) to the Aalenian (Murchisonae Zone p.p.) [Gómez et al., 2003, 2004].

The El Pedregal Formation contains mudstones and bioclastic wackestones to packstones, showing locally interlayered marly beds. The base of the formation shows ferruginous or phosphatic oolites. The biotic content includes microfilaments (fragments of thin-shelled bivalves), echinoids (crinoids), gastropods, oysters, brachiopods, sponges, belemnites, and ammonites. The El Pedregal Formation develops in external and shallow carbonate platform environments affected by storms. Its age ranges from the Aalenian (Murchisonae Zone p.p.) to the end of the Bajocian [Gómez and Fernández-López, 2004].

2.4. *Genetic relationships with surrounding Jurassic volcanism*

Similar and roughly coeval volcanism to that of the Iberian Range has been recorded along the southern Jurassic margin of Iberia in what is now the Median Subbetic domain of the Betic Cordillera [García-Yebra et al., 1972, Vera, 1988, 2001, García-Hernández et al., 1980, Molina et al., 1998, Molina and Vera, 2001, Puga et al., 2004]. Puga et al. [2004] argued that Jurassic basalts and traquibasalts are drawn from fissural volcanism favored by a WSW–ENE trending deep-faulting system.

Volcanic levels are detected from about the Pliensbachian in both the Iberian and Betic basins [Vera et al., 2004, Puga et al., 2011, Gómez et al., 2019, Cortés, 2020]. By contrast, they no longer occur from the early Bajocian (late Laeviuscula Zone or Laeviuscula–Propinquans zonal boundary) in the Iberian carbonate-platform system [Cortés, 2018, 2021], whereas their presence lasted until the Santonian in the Betic Basin [Molina et al., 1998, Molina and Vera, 2008]. Another difference is that lavas, pillow lavas, dikes, and sills were dominant in the Median Subbetic [Gómez et al., 2019] against the pyroclastic explosive deposits that occurred in the Iberian platforms [Cortés, 2018]. All the aforementioned suggests the possibility of volcanisms with a common origin in both basins but maybe reservoirs with different capacity.

3. Materials and methods

3.1. *Primary and secondary volcanic deposits*

There is a need for careful discernment between primary and secondary volcanic deposits to achieve reliable and effective outcomes in the volcanic age estimates. According to White and Houghton [2006] and Sohn and Sohn [2019], primary volcaniclastic deposits are non-reworked ones formed directly from volcanic eruptions (i.e., pyroclastic, autoclastic, hyaloclastic, and peperitic). They contrast with volcaniclastic deposits that are not directly related to eruptions but are reworked, modified, and redeposited by surface or gravitational processes (e.g., tides, waves, currents, or non-eruptive gravitational density flows in the oceanic realm), and are deemed epiclastic or secondary [White and Houghton, 2006].

As cementation of volcaniclastic bodies takes time, primary deposits can be eroded, transported and redeposited several times, resulting in submarine volcanic edifices with mixed primary and epiclastic deposits [e.g., Cortés and Gómez, 2016, 2018]. Their distinction is often problematic, ambiguous, or even impossible, especially for ancient and weathered sites [Cas and Wright, 1987, McPhie et al., 1993, Martínez et al., 1996b, Waitt, 2007, Cas and Giordano, 2014, Sorrentino et al., 2014, Sohn and Sohn, 2019]. Epiclastic layers could be the only relict that provides relevant information about the ancient magmatic activity [Pellenard et al., 1999, 2003, Pellenard and Deconinck, 2006, Sorrentino et al., 2014]; hovewer, they could also be redeposited above sediments post-dating the volcanic event itself.

Elementary criteria for distinguishing between primary and secondary volcanic deposits are:

(1) The presence of continuous lava flows (including pillow lavas) and well-characterized pyroclastic, autoclastic, or hyaloclastic deposits.

(2) Accretionary lapilli are considered as a distinctive feature of primary volcaniclastic deposits [Cas and Wright, 1987, White and Houghton, 2006]. They are described in mainly subaerial pyroclastic fall, surge, and flow deposits, formed by accretion of fine ash around a nucleus [Fisher and Schmincke, 1984, Cas and Wright, 1987]. Indeed, their welded or armored clasts are a diagnostic of subaerial eruptions as pyroclastic flows cannot occur sustainably in aqueous conditions [Fisher and Schmincke, 1984, Kokelaar et al., 1984, Cas and Wright, 1987, De Goër, 2000]. However, it has been suggested that some eruptions of very thick, hot, and dense pyroclastic flows do not mix with ambient water and might keep the heat while being deposited to form subaqueous welded features [Fisher and Schmincke, 1984, Kokelaar and Busby, 1992]. In any case, accretionary lapilli are unequivocal evidence for syn-volcanic hot deposits of either subaerial or, at best, very shallow subaqueous emplacements [Cas and Wright, 1987]. Note that accretionary lapilli can occur as reworked boulders in epiclastic volcanic accumulations far away from the original volcano and primary

deposition point [Fisher and Schmincke, 1984, Cas and Wright, 1987]. To avoid this issue, continuous and non-reworked beds of accretionary lapilli should be considered indicative of primary volcanic deposits.

(3) Even in submarine emplacements, volcanic accumulations can be lithified before being dismantled and, therefore, they can keep their cone morphology. Although the outcrop conditions are not ideal in ancient examples, observing onlapping wedge-shaped sedimentary units over the volcanic surface indicates a pre-existing primary slope.

(4) Observing paleo-vent sites linked to volcanic bodies also constitutes a strong argument for primary volcanic accumulation.

(5) Some volcanic accumulations are not recognizable as volcanic mounds if their decakilometric-sized extent greatly exceeds their height (thickness). Large volumes of volcanic materials distributed over great undersea surfaces could indicate primary volcanic subaqueous emplacements. It is hard to understand how primary volcanic deposits may be remobilized and transported far from the origin and later redeposited on younger substrates as huge epiclastic layers.

3.2. *Field and laboratory work*

The methods used basically consist of fieldwork focused on identifying primary volcanic deposits in order to corroborate the ages of volcanism. To achieve this goal, the geological maps [Cortés, 2018] and each of the 13 volcanic levels along the 20 outcrops of the study area were revisited. Volcanic and carbonate rock types, contacts between sediment beds and volcanic bodies, intravolcanic sediment clasts, isolated intravolcanic fossils, and sedimentary structures and ichnological features within intravolcanic sediment beds, were systematically studied and recorded.

Field observations were supplemented with microfacies studies of thin sections obtained both from beds of well-identified lithological units (formations) and intravolcanic sediment clasts. This additional purpose was to determine the genetic provenance of the intravolcanic clasts and check their potential hot contact relations. Thin sections were prepared at the Complutense University of Madrid (UCM) applying standard techniques, such as staining half of each with alizarin red S and potassium ferrocyanide solution. Thin sections were examined under a Nikon Eclipse E400 Pol polarization light microscope and photographed with a coupled Nikon D7100 (24 megapixels) digital microscope camera at the Department of Stratigraphy of the UCM. Petrographic and sedimentological descriptions were carried out according to the Dunham [1962] and Embry and Klovan [1971] classifications.

Taxonomy and taphonomy of carbonate and volcaniclastic internal molds (ammonoids and brachiopods) were performed by Professors Antonio Goy, Sixto Fernández López, Soledad Ureta (UCM), and José Sandoval (Granada University). Most of this paleontologic material was deposited in the Museo Aragonés de Paleontología, Fundación Dinópolis, Teruel (Spain) under the inventory numbers 201/19 and 206/20.

Some figures of this work have been drafted benefiting from the latest available geographic information (topographic and lidar digital elevation—DEM—maps) in the Instituto Geográfico Nacional (IGN) of Spain. The geographic data were processed and managed with ArcGIS software (generation of hillshade maps from DEM with ArcMAP or 3D landscapes with ArcSCENE) and then edited, when necessary, using AutoCAD or Photoshop software programs.

4. Results and interpretations

4.1. *Primary volcanic deposits*

Lava flows constitute a minority of the total released volcanic products in the studied area. Nevertheless, lava flows have been found in the level V_4 (Caudiel [CA] outcrop), level V_6 (La Puebla de Valverde.4 [PV.4] outcrop), level V_8 (La Puebla de Valverde.2 [PV.2] and La Puebla de Valverde.3 [PV.3] outcrops), and level V_{12} (Caudiel [CA], Sarrión.1 [SA.1], Sarrión.2 [SA.2], and Sarrión.3 [SA.3] outcrops) (Figure 3C,D). Lavas generally make up thin bodies of a short extent, except for the level V_{12} in the Caudiel (CA) outcrop and the level V_8 in the La Puebla de Valverde.3 (PV.3) outcrop. In the volcanic level V_{12} of the Caudiel outcrop, a dome-shaped lava flow (about 520 m long in N–S direction and with a maximum thickness of 12 m) was formed (Figure 4A,B). In the volcanic level V_8 of the La Puebla de Valverde.3 outcrop, a up to

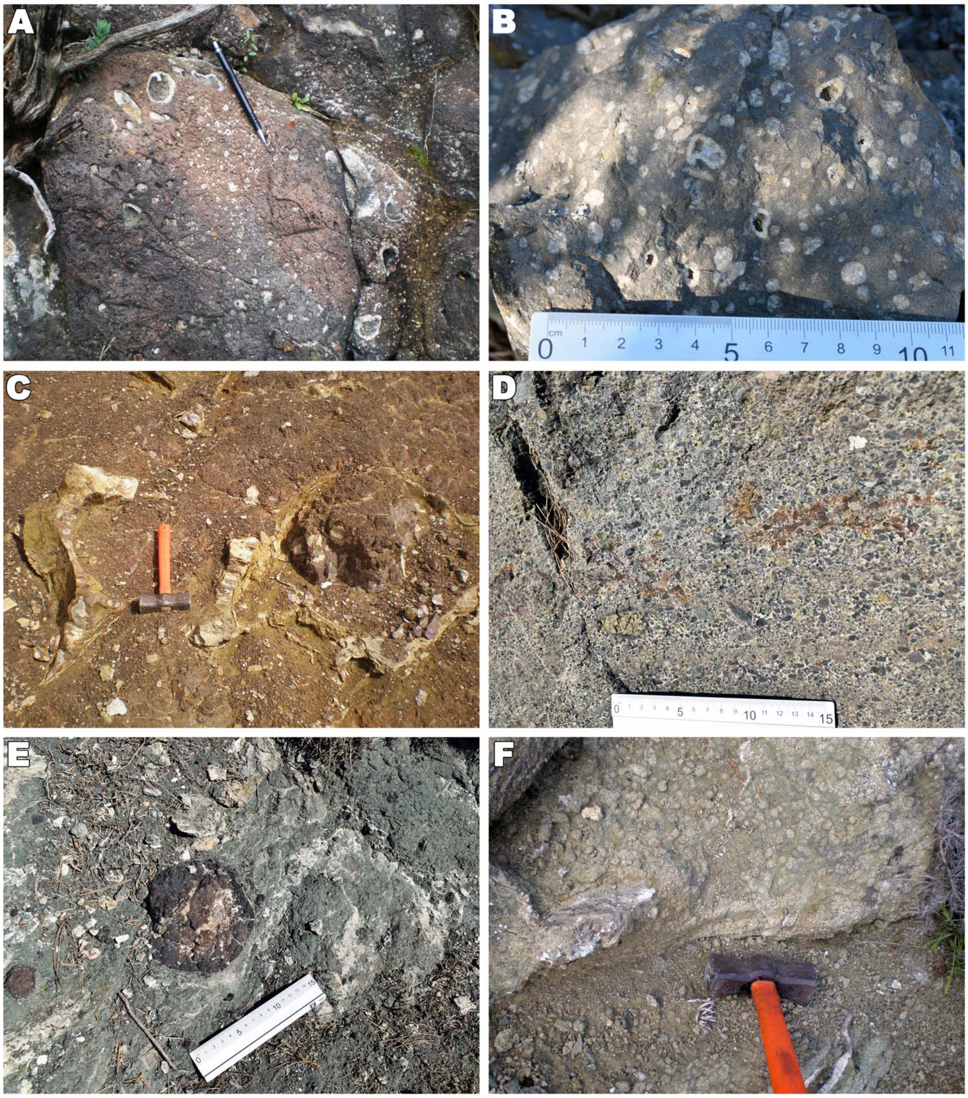

Figure 4. Types of volcanic rocks. (A,B) Lava flows in the Caudiel outcrop (V_{12} volcanic level). (C) Pillow lavas in the La Puebla de Valverde.3 outcrop (volcanic level V_8). (D) Lapilli in the Caudiel outcrop (volcanic level V_{12}). (E) Tuff in the Caudiel outcrop (volcanic level V_{12}). (F) Accretionary lapilli in the Camarena de la Sierra.1 outcrop (volcanic level V_{11}). The pen for scale in (A) is 14 cm long and the hammer in (C) and (F) is 27 cm long.

7 m thick pillow-lavas section has been found (Figure 4C). Well-identified primary pyroclastic deposits (breccia, lapilli, or tuff) have been recognized in all of the studied outcrops (Figure 4D,E), except for the volcanic levels V_1, V_7, and V_{10}. These latter levels do not show lava flows nor pyroclastic, autoclastic, or hyaloclastic features.

Continuous and non-reworked beds of accretionary lapilli have been found throughout the level V_{11} (Camarena de la Sierra.1 [CAM.1] outcrop) (Figures 3C,D, and 4F). The chronostratigraphic position of the volcanic level V_{11} has been linked with an Aalenian (intra-Murchisonae Zone) regional unconformity [Cortés, 2018, 2021]. This unconformity separates the Casinos and El Pedregal formations and corresponds to the boundary between the LJ-4 and MJ-1 second-order transgressive-regressive cycles [Fernández-López, 1997, Fernández-López and Gómez, 2004, Gómez and Fernández-López, 2004, 2006]. The shallow marine conditions of that time are compatible with the water-depth conditions going along welding or above the water-air interface eruptions.

Well-characterized volcanic mounds, as well as volcanic flanks onlapped by younger carbonate beds, have been found in the level V_{11} (Camarena de la Sierra.3 [CAM.3] outcrop), level V_{12} (Caudiel [CA], Pina-Barracas.1 [PI-BA.1], Sarrión.1 [SA.1], Sarrión.2 [SA.2], and Sarrión.3 [SA.3] outcrops), and level V_{13} (Abejuela [AB] and Llíria [LLÍR] outcrops) (Figures 3C,D, and 5).

At least two possible near-vent sites have been identified both in the volcanic level V_9 (Camarena de la Sierra.5 [CAM.5] outcrop) and in the level V_{12} (Caudiel [CA] outcrop). Some features, such as: (i) local breakage able to form subrounded clasts from unconsolidated carbonate beds, probably as a response to the explosive eruption, and (ii) injection of irregular lenses of volcanic matter into the broken sediments, are visible in the volcanic level V_9 from the Camarena de la Sierra.5 (CAM.5) outcrop (Figures 3C,D, and 6A,B,C). Moreover, centimeter- to meter-thick angular calcareous blocks embedded into lava bodies as a result of conduit wall rock fragmentation, partly assimilated and exhibiting peperitic and fluidification textures, are observed in the volcanic level V_{12} from the Caudiel (CA) outcrop (Figure 6D,E). They would correspond to the composite clasts of White and Houghton [2006], formed by the interrelationship between magma and sediment (fragments of peperite).

The most evident large volcanic extents are observed within the volcanic levels V_4, V_5, V_6, V_9, and V_{11} from the La Puebla de Valverde (PV) and Camarena de la Sierra (CAM) outcrops (Figure 3C,D). For example, the volcanic level V_4 in the CAM.1 outcrop shows 2100 m of visible linear length along NE–SW, the volcanic levels V_5 and V_6 in the PV.4 outcrop extend over an area of about 12 km^2, the volcanic level V_9 in the CAM.5 outcrop covers an area of around 5 km^2, and the level V_{11} in the CAM.1 outcrop displays 4500 m of visible linear length in a NE–SW direction. Other large volumes of volcanic deposits, although across more reduced areas, can also be related to the V_2 (Camarena de la Sierra.3 [CAM.3], Camarena de la Sierra.4 [CAM.4], and Camarena de la Sierra.5 [CAM.5] outcrops) and V_3 volcanic levels (Pina-Barracas.2 [PI-BA.2] and Pina-Barracas.3 [PI-BA.3] outcrops). For example, just over 2000 m of visible linear length along NE–SW for the level V_2 in the CAM.5 outcrop, and over 660 m from east to west for the level V_3 in the PI-BA.2 outcrop.

4.2. *Features indicative of secondary volcaniclastic deposits?*

The occurrence of some elements, such as sediment clasts, beds, or fossils within the volcaniclastic piles, could be quoted to argue their secondary epiclastic origin. Whether clasts, fossils, and beds are indicative of secondary volcanic deposits or not is evaluated in the following sub-sections and accompanying figures. Interpretations are based on the results of sedimentological field observations and microfacies analyses.

4.2.1. *Fossils with volcaniclastic infill*

The presence of fossils could be used to postulate reworking in the volcaniclastic deposits. However, it is undeniable that fossils can occur in primary volcaniclastic piles, even in solid basalts [e.g., Nayudu, 1971]. The fossilization happened within the volcanic deposits, and their durability as preserved fossils is estimated as very low but not impossible (Figure 7A,B). The fossil preservation on the superficial levels of the volcanic mass would merely denote fall, shallow burial, and an internal volcanic filling of the shells, but not necessarily reworking processes. However, fossils, especially nektonic ones, found to a certain depth indicate a higher draft in reworking processes. Fossils with volcaniclastic infill will always be more recent than the volcanic body where they are included. Nevertheless, fossil gathering that occurred shortly after the volcanic accumulation may be considered contemporary for most chronostratigraphic dating purposes.

4.2.2. *Sediment clasts*

Sediment clasts included in the volcaniclastic bodies are generally assumed to be fragments of country rocks enclosed and ejected along with the pyroclasts. However, it cannot be ruled out the

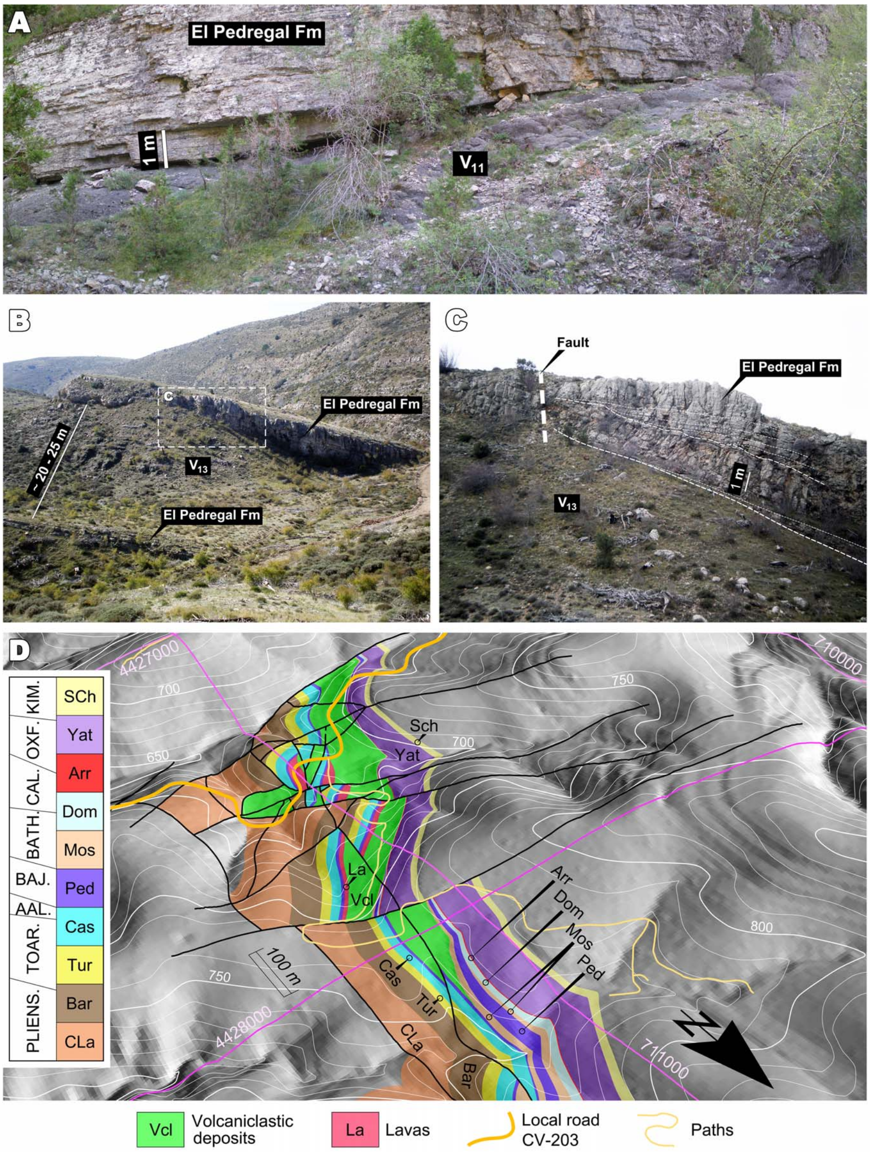

Figure 5. (A) Onlap stratal terminations of the El Pedregal Formation against the flank of a volcanic mound in the Camarena de la Sierra.3 outcrop (volcanic level V_{11}). (B,C) The same in the Abejuela outcrop (volcanic level V_{13}). (D) 3D geological mapping across the northern flank of the volcanic mound in the Caudiel outcrop (volcanic level V_{12}). The El Pedregal, Moscardón, and Domeño formations progressively onlap the volcanic slope. Abbreviations: SCh: Sot de Chera Formation (yellow marls), Yat: Yátova Formation (wackestone–packstones with sponges), Arr: Arroyofrío Bed (wackestone–packstones with ferruginous ooids and pisoids), Dom: Domeño Formation (bioclastic–filaments–wackestone–packstones), Mos: Moscardón Formation (crinoidal packstones to grainstones), Ped: El Pedregal Formation (bioclastic wackestone–packstone with chert nodules), Cas: Casinos Formation (mudstones, bioclastic wackestones, locally packstones, and thin marly beds), Tur: Turmiel Formation (alternation of marls and mudstones to packstones), Bar: Barahona Formation (bioclastic wackestones to packstones, sometime grainstones, with occasional marly beds), CLa: Cuevas Labradas Formation (marls, peritidal mudstones, bioclastic wackestones to packstones, grainstones, and carbonate breccias). PLIENS.: Pliensbachian, TOAR.: Toarcian, AAL.: Aalenian, BAJ.: Bajocian, BATH.: Bathonian, CAL.: Callovian, OXF.: Oxfordian, KIM.: Kimmeridgian.

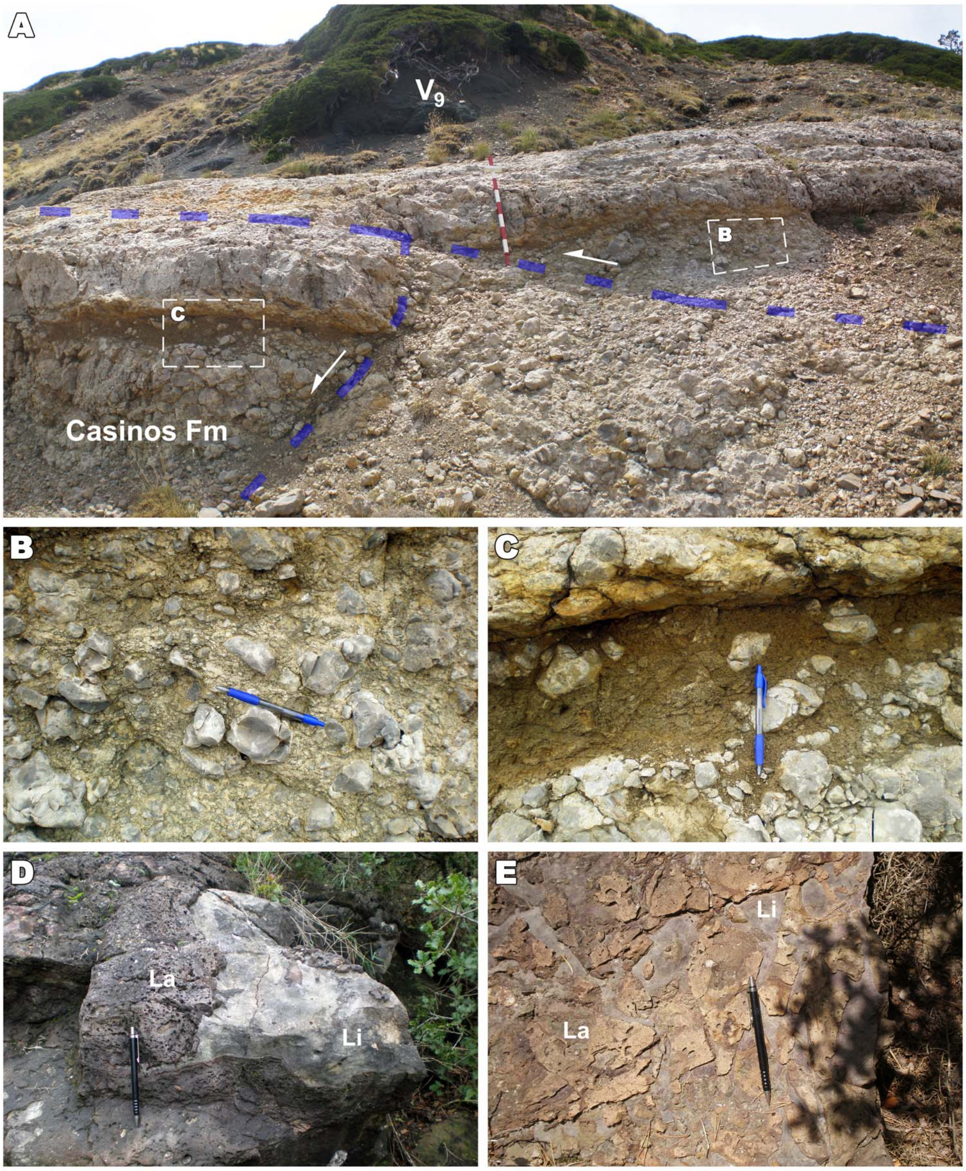

Figure 6. Near-vent sites. (A) Volcanic level V_9 overlying the Casinos Formation in the Camarena de la Sierra.5 (CAM.5) outcrop. Dashed blue lines are faults. (B) Rounded clasts, coming from unconsolidated limestones (Casinos Fm), were probably formed by the effect of explosive eruption processes. (C) Irregular and discontinuous intrusion of volcaniclastic material, including rounded clasts belonging to the Casinos Formation. (D) Centimeter-thick calcareous block partially assimilated by lava flows in the Caudiel outcrop (volcanic level V_{12}). (E) Meter-thick calcareous block in the Caudiel outcrop (related to the volcanic level V_{12}) exhibiting peperitic textures formed while it was still unconsolidated (La: Lava, Li: Limestone). The calcareous blocks in (D) and (E) were probably ripped from the conduit walls and included in the lava bodies in the vicinity of vents. The red and white bar for scale in (A) is 0.90 m in length. The pens for scale in (B)–(E) are 14 cm long.

Figure 7. (A) Bivalves with volcaniclastic infill in the Camarena de la Sierra.1 outcrop (volcanic level V_6). (B) Ammonite specimen with volcaniclastic infill in the Sarrión.2 outcrop (volcanic level V_{12}). (C) Sedimentary clast with chert nodules from the El Pedregal Formation within the volcanic mound (volcanic level V_{13}) in the Abejuela outcrop. (D) Sedimentary clast from the El Pedregal Formation within the volcanic mound (volcanic level V_{13}) in the Abejuela outcrop, containing *Brasilia* sp. (upper part) and *Malladaites* sp. (lower part). (E) Sedimentary clast from the El Pedregal Formation within the volcanic mound (volcanic level V_{13}) in the Abejuela outcrop, containing *Prisnorhynchia rabesaxensis*. (F) Sedimentary clast from the El Pedregal Formation within the volcanic mound (volcanic level V_{13}) in the Abejuela outcrop, containing *Pseudogibbirhynchia mutans*. The pencil for scale in (C) is 14 cm long. Coins of 1 euro for scale in (E) and (F) are 2.3 cm in diameter.

possibility that primary volcaniclastic deposits and pre-existing sediments have been reworked and re-deposited together, resulting in a mixture of volcaniclasts and sedimentary clasts. Thus, their presence within volcaniclastics could support that such volcanic bodies are reworked epiclastic deposits.

Carbonate clasts of sedimentary origin, ranging from a few centimeters to several decimeters in size, are commonly observed all over the volcaniclastic levels from the Pliensbachian to the Bajocian in the studied area. They show high morphologic variability (from subrounded or ellipsoidal to subangular) and often have a recrystallized external appearance along with a frequent concentric black alteration halo.

One of the most exceptional sites concerning the frequency and size variation of intra-volcanic sedimentary clasts is the Abejuela outcrop (volcanic level V_{13}) (Figure 3C,D). Several typical rock types from the pre-volcanic lithostratigraphic units were identified as clasts, as shown by their lithologic features (Figure 7C) and their fossil content (e.g., *Brasilia* sp. along with *Malladaites* sp., *Prisnorhynchia rabesaxensis*, and *Pseudogibbirhynchia mutans*, from the Aalenian) (Figure 7D,E,F).

Thin sections observations indicate that clasts are clearly made of the pre-volcanic units (sometimes much older than the chronostratigraphic position of the volcanic deposit) (Figures 8A–F, 9A–D). They further revealed peperitic textures commonly related to magma intrusions and mingling with the still unconsolidated and wet host sediments. It demonstrates that clasts and magmas were in initial contact (Figure 9E,F).

These observations consistently indicate that the sedimentary clasts included in the volcanic bodies are former wall rocks of volcanic conduits remobilized by explosive volcanic processes. That is, the presence of sediment clasts does not have to be indicative of secondary epiclastic deposits, but rather the opposite.

4.2.3. *Sediment beds*

The presence of centimeter- to meter-thick sedimentary beds included in the volcaniclastic piles requires different consideration than sediment clasts. Detailed observations from these commonly single beds have revealed the widespread occurrence of hummocky cross-stratification (HCS), sedimentary structure typically considered diagnostic of storm deposits in the shallow marine realm [e.g., Dott and Bourgeois, 1982, Hunter and Clifton, 1982, Duke, 1985, Haines, 1988, Monaco, 1992, Sami and Desrochers, 1992, Dumas and Arnott, 2006]. These storm deposits are clearly related to sedimentary processes. Tempestites surrounding volcaniclastic mounds contain clasts of volcanic origin but may also contain fossils. The latter are interpreted to be younger than the volcanic event except if they were reworked from older strata [e.g., reelaborated ammonites of Fernández-López, 1984].

Relationships between primary and secondary volcaniclastic deposits are sometimes found within a single pile: a cm-thick calcareous bed located at the lower and distal part of a volcanic pile can be seen in Figure 10A (Caudiel outcrop). It is made of a bioclastic (mainly bivalves, ammonoids, and crinoids) and intraclastic wackestone–packstone (Figure 10B) interpreted as a tempestite. Intraclasts are volcanic epiclasts. It is overlain by a few meters of volcaniclastic deposits of the same facies as the lower volcanics.

In the La Puebla de Valverde.4 outcrop (Figure 10C), a primary pyroclastic deposit (lapilli) is observed at the lower part of the section (Figure 10D). Above, a cm-thick bed with abundant epiclasts is interpreted as another storm deposit (Figure 10E), covered by fine-grained volcaniclastic deposits with faint traction structures (Figure 10F).

Therefore, since the storm beds (both in Caudiel and La Puebla de Valverde.4 outcrops) are sedimentary in nature, the volcaniclastic material accumulated above them must have been remobilized and redeposited later, as their features and texture often demonstrate, although they are not always easy to distinguish [Cas and Wright, 1987, McPhie et al., 1993, Martínez et al., 1996b, Waitt, 2007, Cas and Giordano, 2014, Sorrentino et al., 2014, Sohn and Sohn, 2019]. The volcaniclastic deposits postdating the storm beds can be interpreted as sliding from the summit of the mounds triggered by the wave activity or collapse mechanisms. In any case, the volcanic section predating the storm beds should be deemed as a primary deposit. Instead, the stretches overlying the sedimentary storm layers are non-primary reworked (epiclastic) products.

In short, it has been established that: (a) both the occurrence of sediment clasts and fossils with

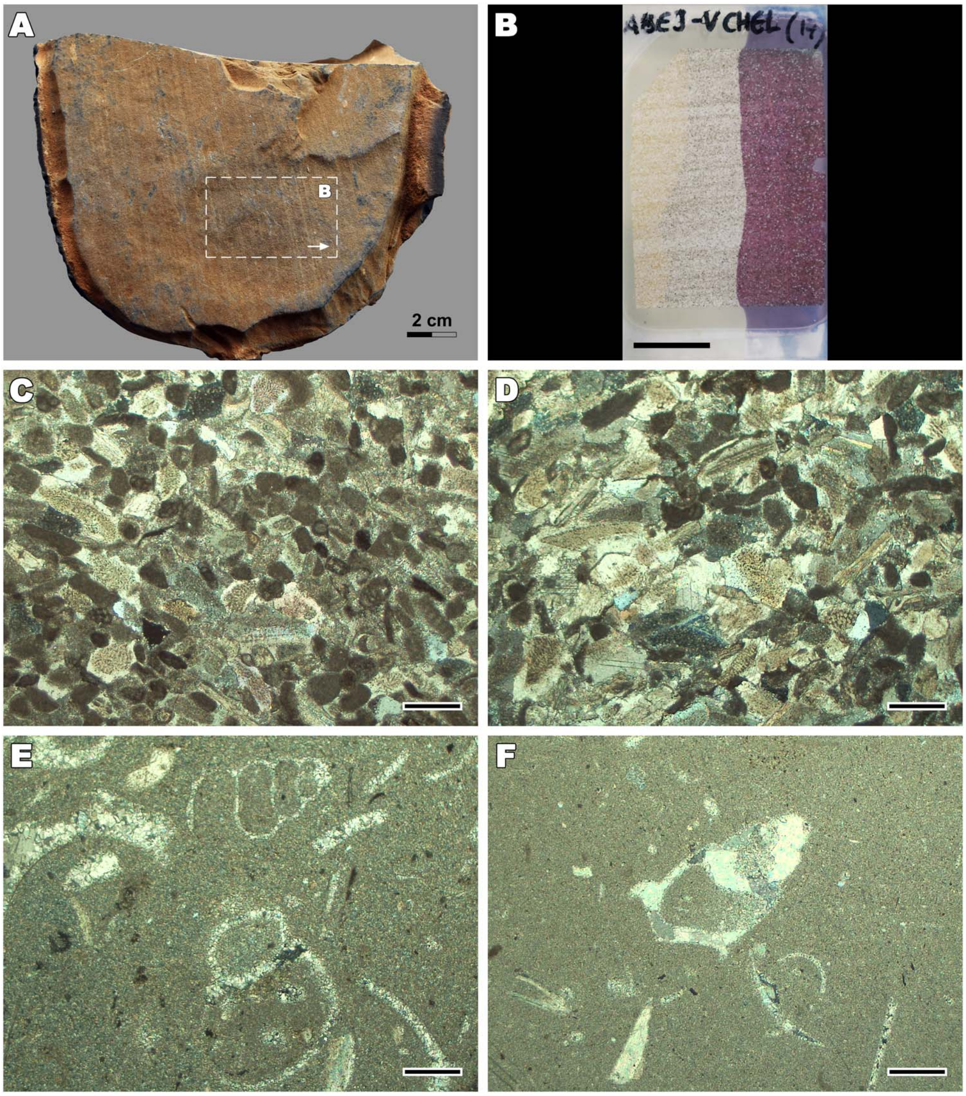

Figure 8. (A) Sedimentary clast probably from the Cuevas Labradas Formation with tractive lamination, included within the volcanic mound (volcanic level V_{13}) in the Abejuela outcrop. (B) Thin section made up of the sedimentary clast photographed in (A). The scale bar corresponds to 1 cm. (C) Microphotograph taken of the thin section (B). It is a well-sorted bioclastic, intraclastic, and peloidal grainstone, showing a grain-supported fabric without micritic matrix. Allochems are packed, and intergranular cement (equal-size spar crystals) is observed. Bioclastic grains are mainly echinoids (crinoid plates), often surrounded by calcitic overgrowths formed in optical continuity (syntaxial rims), and benthic miliolid foraminifera. (D) Similar microphotograph obtained from a high-energy set of subtidal bars belonging to the Cuevas Labradas Formation in the Caudiel outcrop. (E) Microphotograph taken from a thin section of a sedimentary clast included within the volcanic level V_{13} in the Abejuela outcrop. It is a bioclastic wackestone showing a mud-supported fabric where skeletal grains (gastropods) are embedded into a micritic to microsparitic matrix. Original aragonitic shells were dissolved and later filled with sparry calcite. (F) Similar microphotograph coming from the Casinos Formation in the Camarena de la Sierra.3 outcrop. The black scale bars in (C)–(F) correspond to 250 μm. All microphotographs were taken under crossed nicols.

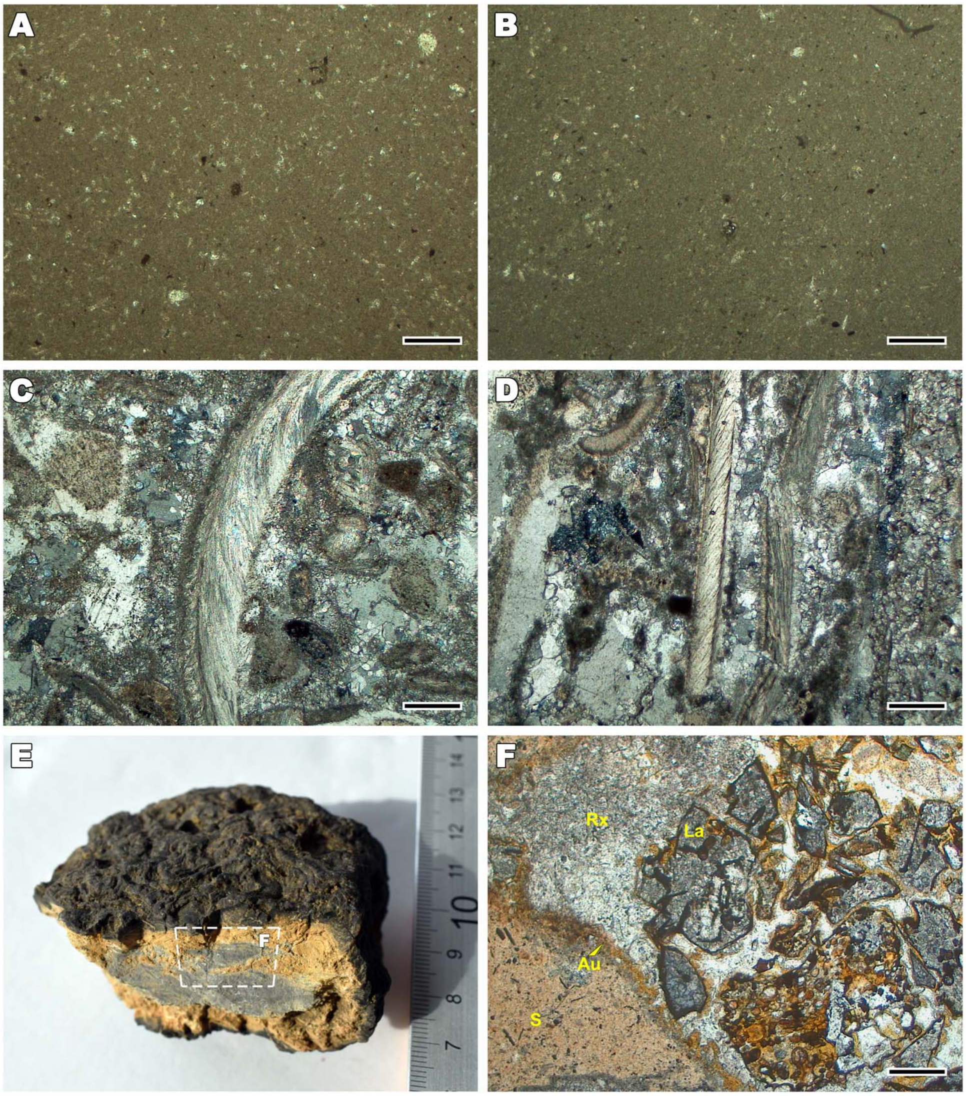

Figure 9. (A) Microphotograph taken from a thin section of a sedimentary clast included within the volcanic level V_3 in the Pina-Barracas.2 outcrop. It is a mudstone with scarce benthic miliolid foraminifera. (B) Similar microphotograph coming from the Cuevas Labradas Formation in the Camarena de la Sierra.3 outcrop. (C) Microphotograph taken from a thin section of a sedimentary clast included within the volcanic level V_4 in the Pina-Barracas.2 outcrop. It is a bioclastic packstone to grainstone with some micritic intraclasts. Main bioclasts are plates of crinoids with syntaxial rims and fragments of thick-shelled bivalves (oysters). (D) Similar microphotograph coming from the Barahona Formation in the La Puebla de Valverde.4 outcrop. (E) Sedimentary clast with a corrugated and dark halo included within the volcanic mound (volcanic level V_{13}) in the Abejuela outcrop. (F) Microphotograph taken from a thin section of the sedimentary clast (E). Note the injection of angular and vesiculated juvenile lava fragments into the sediment resulting in a micropeperite texture. Abbreviations: La: Juvenile lava fragment, Au: Contact aureole surrounding magmatic injection, Rx: Recrystallized calcite, S: unaltered sediment. The black scale bars in (A)–(D), (F) correspond to 250 μm. All microphotographs were taken under crossed nicols, except (F) in plane-polarized light.

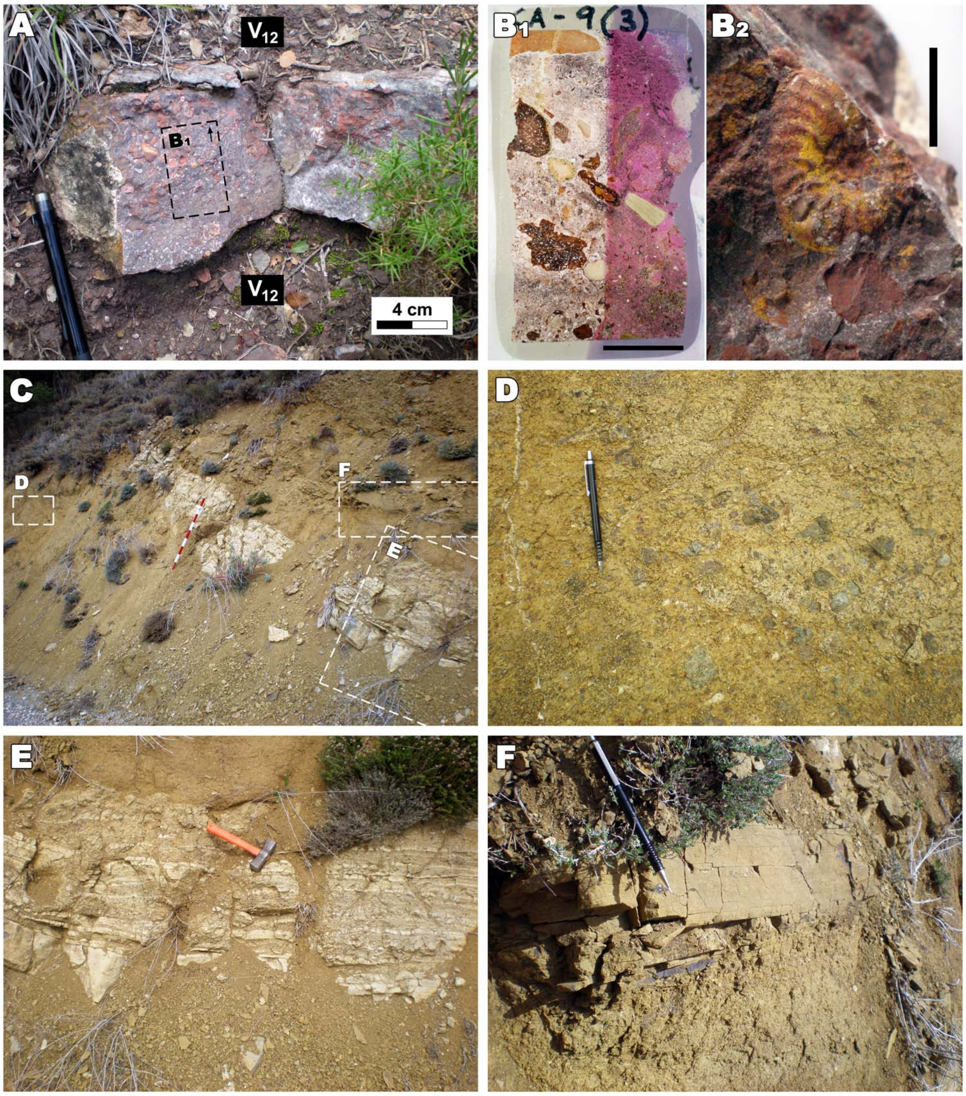

Figure 10. (A) Reddish bioclastic and intraclastic packstone 0.10m thick interpreted as a storm layer, overlying and underlying 1.25 m and 1.85 m, respectively, of volcaniclastic deposits (volcanic level V_{12} in the Caudiel outcrop). (B_1) Thin section made up of the sedimentary bed photographed in (A). Darker intraclasts are lava fragments. (B_2) *Ludwigella* sp. extracted from the intervolcanic storm layer photographed in (A). (C) Volcanic level V_6 in the La Puebla de Valverde.4 outcrop, showing an intervolcanic m-thick sedimentary bed (probably a storm layer). (D) Primary pyroclastic (lapilli) deposit underlying the sedimentary bed. (E) Intervolcanic sedimentary bed. (F) Secondary volcaniclastic (epiclastic) deposit overlying the sedimentary bed. The scale bar in (B_1) and (B_2) corresponds to 1 cm. The red and white bar for scale in (C) is 0.90 m long. The pen in (D) and (F) is 14 cm long. The hammer in (E) is 27 cm long.

volcaniclastic infill is not necessarily indicative of secondary, reworked, and epiclastic deposits, and (b) a sediment layer interbedded within the flank of a volcaniclastic pile clearly marks the boundary between primary (below it) and epiclastic (above it) volcanics.

ZONES / STAGES	VOLCANIC LEVELS	Lavas	Pyroclastic deposits	Vent sites	Mound structures	Armoured lapilli beds	Great volumes
Laeviuscula-Propinquans	V_{13}		LLÍR // AB		LLÍR // AB		
Concavum-Discites	V_{12}	CA // SA.1 // SA.2	CA // PI-BA.1 // SA.1 // SA.2 // SA.3	CA	CA // PI-BA.1 // SA.1 // SA.2 // SA.3		PI-BA.1 // PI-BA.2 // PI-BA.3 // SA.1 // SA.2 // SA.3
Murchisonae	V_{11}		CAM.1		CAM.3	CAM.1	PV.4 // CAM.1 // CAM.3
Thouarsense	V_{10}						
Variabilis	V_9		PV.4 // CAM.4 // CAM.5	CAM.5			PV.4 // CAM.1 // CAM.3 // CAM.4 // CAM.5
Bifrons (Bifrons Subzone)	V_8	PV.2 // PV.3	PV.2 // PV.3				
Bifrons (Sublevisoni Subzone)	V_7						
Serpentinum (Elegantulum Subzone)	V_6	PV.4	PV.2 // PV.3 // PV.4 // CAM.1 // CAM.2 // CAM.4				PV.2 // PV.3 // PV.4 // CAM.1 // CAM.2 // CAM.3 // CAM.4
Serpentinum (Elegantulum Subzone)	V_5		PV.2 // PV.3 // PV.4 // CAM.1 // CAM.4				PV.2 // PV.3 // PV.4 // CAM.1 // CAM.2 // CAM.3 // CAM.4 // CAM.5
Spinatum	V_4	CA	CA // PI-BA.2 // PV.5 // CAM.1				PV.4 // CAM.1 // CAM.3 // CAM.5
late Pliensbachian (Spinatum?)	V_3		PI-BA.2				PI-BA.2 // PI-BA.3
late Pliensbachian	V_2		CAM.4				CAM.3 // CAM.4 // CAM.5
early Pliensbachian (Jamesoni or later)	V_1						

OUTCROPS

CA: CAUDIEL
PI-BA.1: PINA-BARRACAS.1
PI-BA.2: PINA-BARRACAS.2
PI-BA.3: PINA-BARRACAS.3
SA.1: SARRIÓN.1
SA.2: SARRIÓN.2
SA.3: SARRIÓN.3
LLÍR: LLÍRIA
AB: ABEJUELA
PV.2: LA PUEBLA DE VALVERDE.2
PV.3: LA PUEBLA DE VALVERDE.3
PV.4: LA PUEBLA DE VALVERDE.4
CAM.1: CAMARENA DE LA SIERRA.1
CAM.2: CAMARENA DE LA SIERRA.2
CAM.3: CAMARENA DE LA SIERRA.3
CAM.4: CAMARENA DE LA SIERRA.4
CAM.5: CAMARENA DE LA SIERRA.5

Figure 11. Application of the criteria that assist in identifying primary volcanic episodes. Almost all the volcanic levels accomplish one or more criteria in one or several outcrops, except for the levels V_1, V_7, and V_{10}.

5. Discussion

5.1. *Stratigraphic ages of volcanic deposits and timing of volcanism*

The analysis of volcanic deposits according to diagnostic criteria for primary volcanic deposits is summarized in Figure 11. As can be seen, most of the 13 volcanic levels must be witnesses of primary volcanism. Almost all of them meet one or several criteria in one or more outcrops. The exceptions are the volcanic levels V_1, V_7, and V_{10} because they do not meet any of the above criteria. These three volcanic levels show in all of the outcrops and across their entire thickness a mixture of volcanic and non-volcanic components (thin mud-carbonate drapes separating uneven or lenticular volcanic debris, Figure 12A, thin lenticular beds of mudstone with plane parallel lamination, Figure 12B), tractional sedimentary structures (undulate stratification with bioclastic and sedimentary particles, Figure 12C, cross and planar lamination, Figure 12D), complete invertebrate marine fossils embedded in the volcano-sedimentary groundmass, and hallmarks of bioturbation.

They are portions derived from volcanic edifices either preserved in the subsurface or already entirely eroded, with the doubt as to whether they are coeval or more recent than the volcanism age.

The volcanic level V_7 occurs across the Camarena de la Sierra.5 (CAM.5) outcrop, reaching only a centimetric thickness where it crops out. The same thicknesses are observed for volcanic level V_{10}, present in the La Puebla de Valverde.4 (PV.4) and Sarrión.3 (SA.3) outcrops. It could be argued that V_{10} is reworked from the volcanic level V_9 in the La Puebla de Valverde.4 (PV.4) outcrop but cannot be demonstrated for the Sarrión.3 (SA.3) outcrop where V_9 is not observed. Finally, the volcanic level V_1 has only been locally recorded in the Camarena de la Sierra.4 (CAM.4) outcrop. If its volcano-sedimentary origin is assumed, the occurrence of an older volcanic phase should be investigated but is not confirmed by outcrops.

Since the youngest volcanic level (V_{13}) verifies several criteria for a primary volcanic deposit, the resulting period of volcanism spans the early Pliensbachian (or a bit older) to the early Bajocian. The number of syn-eruptive volcanic phases would correspond with the number of interbedded

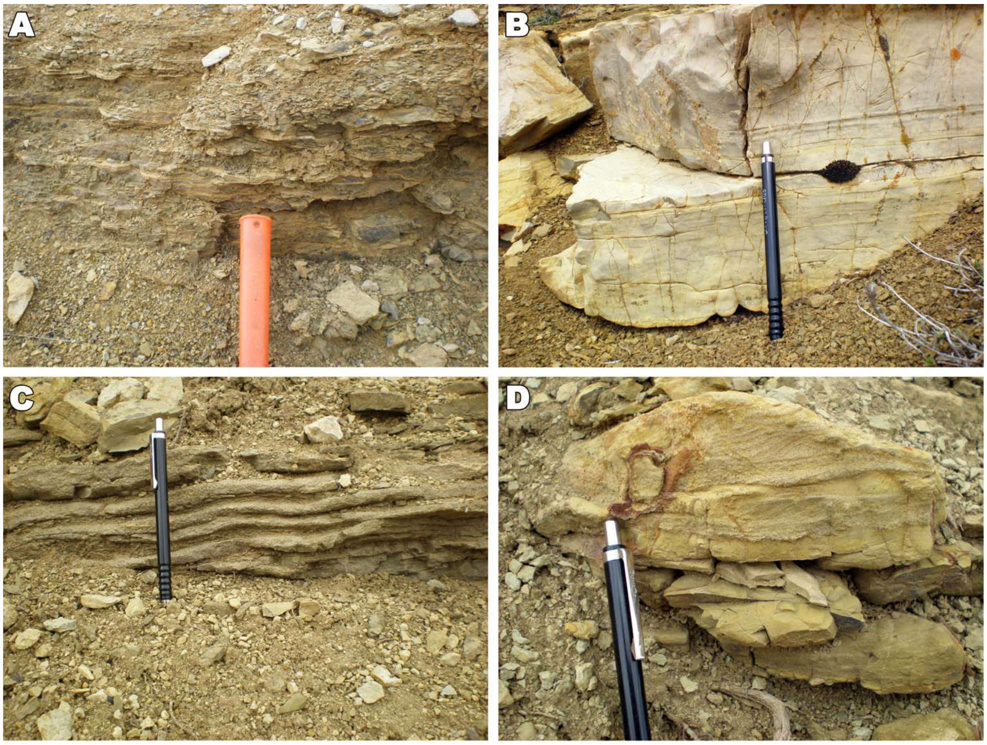

Figure 12. Volcano-sedimentary features from the volcanic level V_7 in the CAM.5 outcrop. (A) Multiple millimeter-sized calcareous lenses intercalated within fine-grained volcano-sedimentary materials. (B) Faint plane-parallel laminated mudstone within the volcanic pile. (C) Centimeter-sized undulated layers of volcano-sedimentary lapilli tuffs intercalated with more fine-grained millimeter-sized epiclastic lutites. (D) Coarser cross-bedded tractional intervals capped by fine-grained interbeds of volcano-lutites. The pen in (B) and (C) is 14 cm long. The visible part of the pen in (D) is about 8 cm long. The visible part of the hammer in (A) is about 17 cm long.

volcanic deposits (i.e., 13) or slightly lower (possibly between 10 and 12, if one, two, or all three levels in question—V_1, V_7, V_{10}—do not represent actual volcanic events).

5.2. *Spatio-temporal sequence of volcanic emissions along structural trends*

The Jurassic volcanic activity (early Pliensbachian–early Bajocian) is supposed to develop in a post-rift or passive margin stage [Salas et al., 2001, Gómez et al., 2019] and therefore in a tectonic quiescence period with decreasing subsidence rates. However, Gómez [1979], Fernández-López and Gómez [2004], Gómez et al. [2004], Gómez and Goy [2005], Gómez and Fernández-López [2006], and Gómez et al. [2019] noticed the presence of two systems of NW–SE and NE–SW trending faults active during the Early and Middle Jurassic through the central and southern Iberian Range, which delimited depocenters and topographic highs.

An additional rift pulse associated with magmatism is referred by Van Wees et al. [1998], who claimed that the number of rifting pulses of low magnitude is much higher than was usually estimated. A period of rapid tectonic subsidence during the Pliensbachian–Toarcian interval would be followed by decreasing subsidence rates from the Aalenian to the Oxfordian. Although neglected in other studies, much of the magmatic early Pliensbachian–early Bajocian time interval falls within it.

Regional mapping [Gautier, 1974, Abril et al., 1975, 1978, Campos et al., 1977, Lazuen and Roldán, 1977, Adrover et al., 1983] demonstrates that the volcanic rocks are emplaced along three of the mentioned linear structural discontinuities, two NW–SE trending faults [Caudiel and Alcublas fault zones, Gómez, 1979] and one oriented NE–SW [Teruel Fault Zone, Fernández-López and Gómez, 2004] (Figure 3C). It might be speculated that the NW–SE oriented Caudiel and Alcublas fault zones could be laterally connected to the Ligurian mid-ocean ridge axis by transform faults. By contrast, the NE–SW (or NNE–SSW) Teruel Fault Zone runs roughly orthogonal to the Jurassic extensional direction.

Based on the biostratigraphic dating carried out by Cortés [2018, 2020, 2021], Figure 13 shows the spatial distribution of the subaqueous emission centers that change along time. The volcanism mostly focused on the Teruel Fault Zone during the Early and earliest Middle Jurassic, being sporadically recorded towards the Caudiel Fault Zone, such as the volcanic episodes V_3, V_4, and V_{11} (Figure 13).

This spatial distribution changed during the Middle Jurassic. The active volcanism migrated southeastward from the Teruel Fault Zone to the Caudiel Fault Zone during the emplacement of the volcanic episode V_{12} (Aalenian–Bajocian, Concavum–Discites, boundary in age).

Then, the volcanism migrated southwards from the Caudiel Fault Zone to the Alcublas Fault Zone. It is not until the uppermost Laeviuscula Zone or the Laeviuscula–Propinquans zonal boundary that the Alcublas Fault Zone underwent magmatic activity with the emission of the volcanic episode V_{13}, which appears solely arranged along this fault zone (Figure 13).

5.3. *Geodynamic context of the Jurassic magmatism within the Iberian Range*

Intraplate magmatism is, in principle, hard to explain within the frame of plate tectonics [Farnetani and Hofmann, 2011, Lee and Grand, 2012]. There is general agreement that intraplate volcanism is triggered by decompression melting and related to deep mantle processes—plumes (hotspots)—, although perhaps not as deep as initially thought [Foulger and Natland, 2003], or off-axis magmatism.

The volcanism recorded in the Iberian Range meets a number of requests on the specifics of hotspots and off-axis magmatism, such as intraplate setting, basalts enriched in incompatible elements (e.g., Perfit and Davidson [2000]), or magmatic crustal penetration controlled by crustal structures such as fault systems [e.g., Mutschler et al., 1998].

Typical off-axis magmatism develops over oceanic crust on the faulted flanks of mid-ocean ridges [e.g., Sohn and Sims, 2005, Canales et al., 2012, Toomey, 2012, Carbotte et al., 2012, 2016, Choi et al., 2021]. Off-axis magmatism has been reported as occurring up to 20 km beyond the ridge axis in the East Pacific Rise [Turner et al., 2011], up to 40 km in the Gulf of Aden [Guillard et al., 2021], or by more than 200 km in the volcanic fields of the Kamar-Daban, the Udokan and the Vitim Plateau [Yang et al., 2018].

Longer distances than those mentioned could undoubtedly separate the studied area from the Ligurian mid-ocean ridge. Moreover, the studied area locates over the rifted continental crust. This suggests that the Jurassic volcanism of the Iberian Range might be originated from hotspot magmatism (Figure 1). The Iberian magmatic region, located at the junction between the Betic and Ligurian basins, constituted a zone of diffuse continental extension that recorded distributed phases of rift until Late Cretaceous times [Angrand et al., 2020]. This scenario, also supported by Van Wees et al. [1998] for the Pliensbachian–Toarcian interval, could have encouraged the rise and extrusion of magma. The lack of magmatism during the second Mesozoic Iberian rifting stage—from the Callovian–Oxfordian boundary [Gómez et al., 2019] or the latest Oxfordian [Salas and Casas, 1993, Salas et al., 2001, Sánchez-Moya and Sopeña, 2004] to the Albian—could be tentatively explained by magmatic chamber depletion. However, it is somewhat paradoxical that magmatism was present in the Iberian Basin during a generally agreed inter-rifting stage.

6. Conclusions

Using biochronostratigraphic methods applied in sediments hosting volcanic bodies to date volcanic events is effective when there is a good record of fossils with chronostratigraphic value, such as ammonites. The results can be applied to other problematic dating cases or to double-check for existing dating. It is essential to keep in mind that some volcanic levels might not match exactly with any volcanic event but that they would have been eroded from the prime accumulation and redeposited on

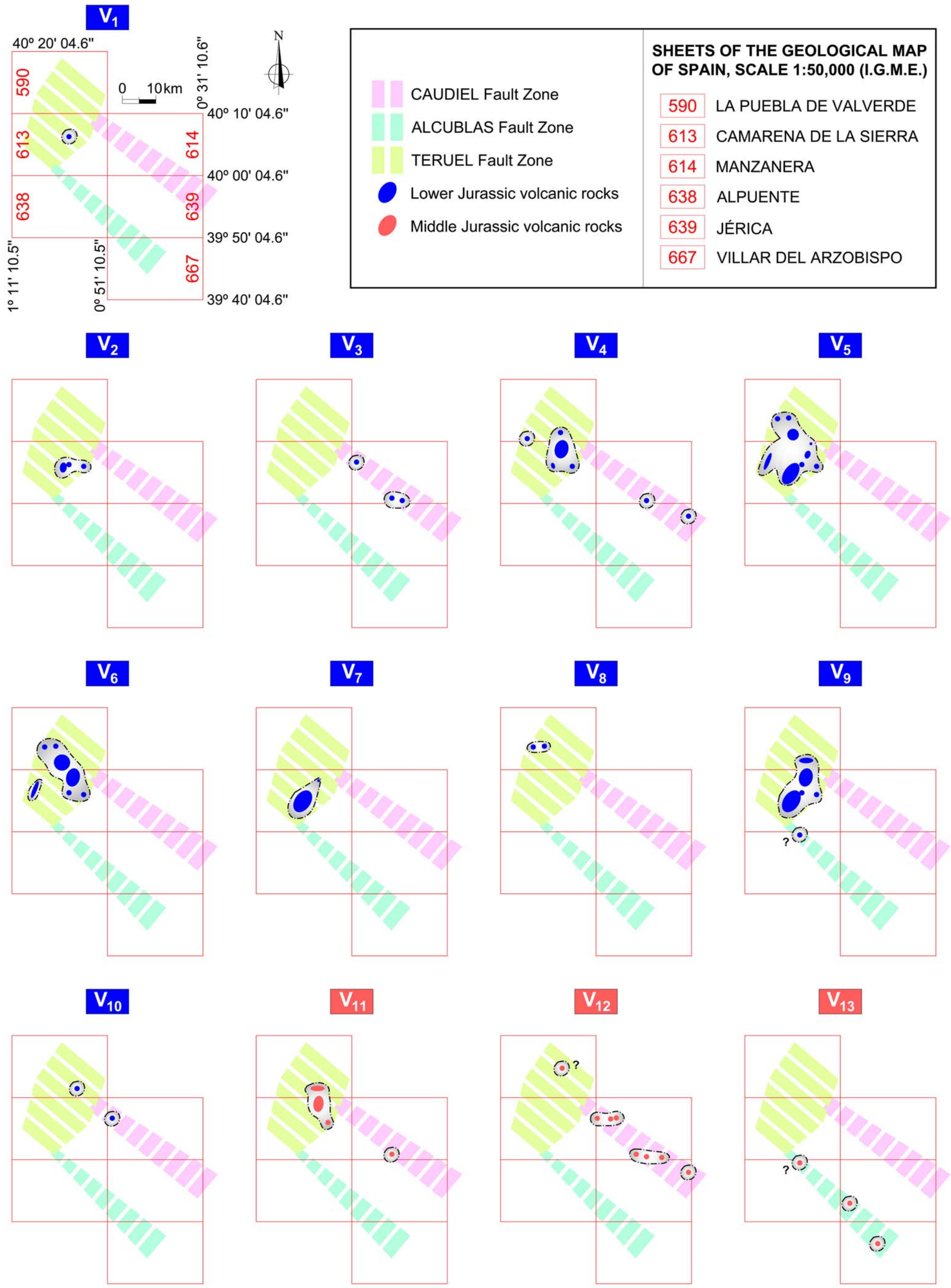

Figure 13. Geographic distribution of the volcanic episodes along the fault zones over time.

younger substrates than those in which they were primarily stored.

The implementation of field criteria as tools for the identification of primary volcanic accumulations has made it possible to establish a reliable time interval for the Jurassic volcanism (ca. 20 Ma) in the southeastern Iberian Range, at zone or even subzone ammonite scale: from the early Pliensbachian

(Jamesoni Zone or later) to the early Bajocian (uppermost Laeviuscula Zone or Laeviuscula–Propinquans zonal boundary). It unlocked the possibility to discuss the spatio-temporal migration of active volcanism at the scale of the study area.

Through precise dating of volcanic episodes, it can be observed that the timing of magmatic eruptions was not simultaneous in the three Fault Zones affecting the area. Exceptionally, the emission of volcanic products becomes synchronous in two of them. Furthermore, what has been noticed is that the volcanic outcrops are shown grouped around preferred locations that change over time. Firstly, it shifted towards the southeast from the Teruel Fault Zone to the Caudiel Fault Zone around the Aalenian–Bajocian boundary and then southward (or towards the SSW) from the Caudiel Fault Zone to the Alcublas Fault Zone around the early Bajocian (uppermost Laeviuscula Zone or Laeviuscula–Propinquans zonal boundary).

Conflicts of interest

The author has no conflict of interest to declare.

Acknowledgments

Thanks to Antonio Goy Goy, Sixto Fernández López, and José Sandoval Gabarrón for the taxonomic determination of the brachiopod and ammonite specimens referred in this work. The author would like to thank the useful comments, suggestions, and revisions of Emmanuel Masini and two anonymous reviewers, which contributed to a much improved paper. The careful editorial handling of Michel Campillo is greatly appreciated.

References

Abril, J., Apalategui, O., Ferreiro, E., García, F., González, F., Hernández, E., Lago, E., Ortí, F., Pliego, D. V., Quintero, I., and Rubio, J. (1978). *Mapa Geológico de España 1:50,000 (2nd Series), Sheet No. 613 (Camarena de la Sierra).* IGME, Madrid.

Abril, J., García, F., González, F., Iglesias, M., Ortí, F., and Rubio, J. (1975). *Mapa Geológico de España 1:50,000 (2nd Series), Sheet No. 638 (Alpuente).* IGME, Madrid.

Adrover, R., Aguilar, M. J., Alberdi, M. T., Aragonés, E., Aznar, J. M., Comas, M. J., Gabaldón, V., Giner, J., Godoy, A., Goy, A., Gutiérrez, M., Leal, M. C., Moissenet, E., Olivé, A., Portero, J. M., Ramírez, J. I., and Ramírez del Pozo, J. (1983). *Mapa Geológico de España 1:50,000 (2nd Series), Sheet No. 590 (La Puebla de Valverde).* IGME, Madrid.

Ancochea, E., Muñoz, M., and Sagredo, J. (1988). Identificación geoquímica del vulcanismo Jurásico de la Cordillera Ibérica. *Geociências (Aveiro)*, 3(1-2), 15–22.

Angrand, P. and Mouthereau, F. (2021). Evolution of the Alpine orogenic belts in the Western Mediterranean region as resolved by the kinematics of the Europe-Africa diffuse plate boundary. *Bull. Soc. Géol. Fr.-Earth Sci. Bull.*, 192, article no. 42.

Angrand, P., Mouthereau, F., Masini, E., and Asti, R. (2020). A reconstruction of Iberia accounting for Western Tethys–North Atlantic kinematics since the late-Permian–Triassic. *Solid Earth*, 11, 1313–1332.

Berra, F. and Angiolini, L. (2014). The evolution of the Tethys region throughout the Phanerozoic: A brief tectonic reconstruction. In Marlow, L., Kendall, C., and Yose, L., editors, *Petroleum Systems of the Tethyan Region*, American Association of Petroleum Geologists Memoir 106, pages 1–27. AAPG, Tulsa, OK.

Blakey, R. (2011). *Paleogeography of Europe Series. Deep Time Maps.* Retrieved in June 2022, from https://www.deeptimemaps.com/map-room/.

Callomon, J. H. (2003). The Middle Jurassic of western and northern Europe: its subdivisions, geochronology and correlations. *Geol. Surv. Denmark Greenland Bull.*, 1, 61–73.

Campos, C., González, F., Goy, A., Lazuen, J., Martín, P., and Ortí, F. (1977). *Mapa Geológico de España 1:50,000 (2nd Series), Sheet No. 639 (Jérica).* IGME, Madrid.

Canales, J. P., Carton, H., Carbotte, S. M., Mutter, J. C., Nedimović, M. R., Xu, M., Aghaei, O., Marjanović, M., and Newman, K. (2012). Network off-axis melt bodies at the East Pacific Rise. *Nat. Geosci.*, 5, 279–283.

Carbotte, S. M., Canales, J. P., Nedimović, M. R., Carton, H., and Mutter, J. C. (2012). Recent seismic studies at the East Pacific Rise 8°20’–10°10’N and Endeavour segment: insights into mid-ocean ridge hydrothermal and magmatic processes. *Oceanography*, 25(1), 100–112.

Carbotte, S. M., Smith, D. K., Cannat, M., and Klein, E. M. (2016). Tectonic and magmatic segmentation of the Global Ocean Ridge System: a synthesis of observations. In Wright, T. J., Ayele, A., Ferguson, D. J., Kidane, T., and Vye-Brown, C., editors, *Magmatic Rifting and Active Volcanism*, Geological Society London Special Publications 420, pages 249–295. Geological Society of London.

Cas, R. A. F. (1992). Submarine volcanism: Eruption styles, products, and relevance to understanding the host-rock successions to volcanic-hosted massive sulfide deposits. *Econ. Geol.*, 87(3), 511–541.

Cas, R. A. F. and Giordano, G. (2014). Submarine volcanism: a review of the constraints, processes and products, and relevance to the Cabo de Gata volcanic succession. *Ital. J. Geosci.*, 133(3), 362–377.

Cas, R. A. F. and Wright, J. V. (1987). *Volcanic successions Modern and Ancient.* Chapman and Hall, London.

Choi, H., Kim, S.-S., Park, S.-H., and Kim, H. J. (2021). Geomorphological and spatial characteristics of underwater volcanoes in the easternmost Australian–Antarctic ridge. *Remote Sens.*, 13(5), article no. 997.

Cohen, K. M., Finney, S. C., Gibbard, P. l., and Fan, J.-X. (2013). The ICS international chronostratigraphic chart. *Episodes*, 36(3), 199–204. https://stratigraphy.org/chart.

Copeland, P. (2020). On the use of geochronology of detrital grains in determining the time of deposition of clastic sedimentary strata. *Basin Res.*, 32(6), 1532–1546.

Cortés, J. E. (2018). *La arquitectura deposicional de los carbonatos del Jurásico Inferior y Medio relacionados con los materiales volcánicos del sureste de la Cordillera Ibérica.* PhD thesis, Universidad Complutense, Madrid, https://eprints.ucm.es/id/eprint/56088/.

Cortés, J. E. (2020). Volcanic rocks in Lower Jurassic marine carbonate successions in the southeastern Iberian Range (Spain): biochronostratigraphic dating. *J. Iber. Geol.*, 46(3), 253–277.

Cortés, J. E. (2021). Using high-resolution ammonite biochronostratigraphy to date volcanogenic deposits preserved in Middle Jurassic carbonate platforms successions of the westernmost Tethys (Southeastern Iberian Range, Spain). *Riv. Ital. Paleontol. Stratigr.*, 127(3), 557–583.

Cortés, J. E. and Gómez, J. J. (2016). Middle Jurassic volcanism in a magmatic-rich passive margin linked to the Caudiel Fault Zone (Iberian Range, East of Spain): biostratigraphical dating. *J. Iber. Geol.*, 42(3), 335–354.

Cortés, J. E. and Gómez, J. J. (2018). The epiclastic barrier-island system of the Early–Middle Jurassic in eastern Spain. *J. Iber. Geol.*, 44(2), 257–271.

De Goër, A. (2000). Peperites from the Limagne Trench (Auvergne, French Massif Central): A distinctive facies of phreatomagmatic pyroclastics. History of a semantic drift. In Leyrit, H. and Montenat, C., editors, *Volcaniclastic Rocks from Magmas to Sediments*, pages 91–110. Gordon and Breach Science Publishers, London.

Dott, Jr., R. H.. and Bourgeois, J. (1982). Hummocky stratification: Significance of its variable bedding sequences. *Geol. Soc. Am. Bull.*, 93(8), 663–680.

Duke, W. L. (1985). Hummocky cross-stratification, tropical hurricanes, and intense winter storms. *Sedimentology*, 32(2), 167–194.

Dumas, S. and Arnott, R. W. C. (2006). Origin of hummocky and swaley cross-stratification—The controlling influence of unidirectional current strength and aggradation rate. *Geology*, 34(12), 1073–1076.

Dunham, R. J. (1962). Classification of carbonate rocks according to depositional texture. In Ham, W. E., editor, *Classification of Carbonate Rocks*, American Association of Petroleum Geologists Memoir 1, pages 108–121. AAPG, Tulsa, OK.

Embry, A. F. and Klovan, J. E. (1971). A Late Devonian reef tract on Northeastern Banks Island, NWT. *Can. Pet. Geol. Bull.*, 19, 730–781.

Farnetani, C. G. and Hofmann, A. W. (2011). Mantle plumes. In Gupta, H. K., editor, *Encyclopedia of Solid Earth Geophysics*, pages 857–869. Springer, Berlin.

Fernández-López, S. (1984). Criterios elementales de reelaboración tafonómica en ammonites de la Cordillera Ibérica. *Acta Geol. Hispánica*, 19(2), 105–116.

Fernández-López, S. (1997). Ammonites, taphonomic cycles and stratigraphic cycles in carbonate epicontinental platforms. *Cuad. Geol. Ibérica*, 23, 95–136.

Fernández-López, S. and Gómez, J. J. (2004). The Middle Jurassic Eastern margin of the Iberian platform system (eastern Spain). Palaeogeography and biodispersal routes of ammonoids. *Riv. Ital. Paleontol. Stratigr.*, 110(1), 151–162.

Fernández-López, S. R. (1985). *El Bajociense en la Cordillera Ibérica. I.—Taxonomía y Sistemática (Ammonoidea). II.—Bioestratigrafía. III.—Atlas.* PhD thesis, Universidad Complutense, Madrid.

Fisher, R. V. and Schmincke, H.-U. (1984). *Pyroclastic Rocks.* Springer-Verlag, Berlin.

Foulger, G. R. and Natland, J. H. (2003). Is "hotspot" volcanism a consequence of plate tectonics? *Science*, 300(5621), 921–922.

García-Hernández, M., López-Garrido, A. C., Rivas, P., Sanz de Galdeano, C., and Vera, J. A. (1980). Mesozoic palaeogeographic evolution of the External Zones of the Betic Cordillera. *Geol. Mijnb.*, 59(2), 155–168.

García-Yebra, R., Rivas, P., and Vera, J. A. (1972). Precisiones sobre la edad de las coladas volcánicas jurásicas en la región Algarinejo-Lojilla (Zona Subbética). *Acta Geol. Hispánica*, VII(5), 133–137.

Gautier, F. (1968). Sur l'existence et l'age d'un paléovolcanisme dans le Jurassique sud-aragonais (Espagne). *C. R. Somm. Séances Soc. Géol. Fr.*, 3, 74–75.

Gautier, F. (1974). *Mapa Geológico de España 1:50,000 (2nd Series), Sheet No. 614 (Manzanera).* IGME, Madrid.

Gómez, J. J. (1979). *El Jurásico en Facies Carbonatadas del Sector Levantino de la Cordillera Ibérica. Seminarios de Estratigrafía.* Serie Monografías 4. Universidad Complutense de Madrid-Consejo Superior de Investigaciones Científicas, Madrid.

Gómez, J. J., Comas-Rengifo, M., and Goy, A. (2003). Las unidades litoestratigráficas del Jurásico Inferior de las Cordilleras Ibérica y Costeras Catalanas. *Rev. Soc. Geol. España*, 16(3–4), 227–238.

Gómez, J. J. and Fernández-López, S. (2004). Las unidades litoestratigráficas del Jurásico Medio de la Cordillera Ibérica. *Geogaceta*, 35, 91–94.

Gómez, J. J. and Fernández-López, S. (2006). The Iberian Middle Jurassic carbonate-platform system: Synthesis of the palaeogeographic elements of its eastern margin (Spain). *Palaeogeogr. Palaeoclimatol. Palaeoecol.*, 236(3–4), 190–205.

Gómez, J. J., Fernández-López, S., and Goy, A. (2004). Primera fase de post-rifting: Jurásico Inferior y Medio. In Vera, J. A., editor, *Geología de España*, pages 495–503. Sociedad Geológica de España-Instituto Geológico y Minero de España (SGE-IGME), Madrid.

Gómez, J. J. and Goy, A. (2000). Definition and organization of limestone-marl cycles in the Toarcian of the northern and east-central part of the Iberian Subplate (Spain). *GeoRes. Forum*, 6, 301–310.

Gómez, J. J. and Goy, A. (2005). Late Triassic and Early Jurassic palaeogeographic evolution and depositional cycles of the Western Tethys Iberian platform system (Eastern Spain). *Palaeogeogr. Palaeoclimatol. Palaeoecol.*, 222(1–2), 77–94.

Gómez, J. J., Sandoval, J., Aguado, R., O'Dogherty, L., and Osete, M. L. (2019). The Alpine Cycle in eastern Iberia: microplate units and geodynamic stages. In Quesada, C. and Oliveira, J. T., editors, *The Geology of Iberia: A Geodynamic Approach. Volume 3: The Alpine Cycle*, pages 15–27. Springer Nature, Heidelberg.

Goy, A., Gómez, J., and Yébenes, A. (1976). El Jurásico de la rama castellana de la Cordillera Ibérica (Mitad Norte). I. Unidades litoestratigráficas. *Estud. Geol.*, 32, 391–423.

Gradstein, F. M., Ogg, J. G., Schmitz, M. D., and Ogg, G. M. (2012). *The Geologic Time Scale.* Elsevier, Amsterdam.

Guillard, M., Leroy, S., Cannat, M., and Sloan, H. (2021). Margin-to-margin seafloor spreading in the Eastern Gulf of Aden: A 16 Ma-long history of deformation and magmatism from seismic reflection, gravity and magnetic data. *Front. Earth Sci.*, 9, article no. 707721.

Haines, P. W. (1988). Storm-dominated mixed carbonate/siliciclastic shelf sequence displaying cycles of hummocky cross-stratification, late Proterozoic Wonoka Formation, South Australia. *Sediment. Geol.*, 58(2–4), 237–254.

Hunter, R. E. and Clifton, H. E. (1982). Cyclic deposits and hummocky cross stratification of probable storm origin in Upper Cretaceous rocks of the Cape Sebastian area, southwestern Oregon. *J. Sediment. Petrol.*, 52(1), 127–143.

Kokelaar, B. P., Howells, M. F., Bevins, R. E., and Roach, R. A. (1984). Volcanic and associated sedimentary and tectonic processes in the Ordovician marginal basin of Wales: a field guide. In Kokelaar, B. P. and Howells, M. F., editors, *Marginal Basin Geology: Volcanic and Associated Sedimentary and Tectonic Processes in Modern and Ancient Marginal*

Basins, Geological Society London Special Publications 16, pages 291–322. Geological Society of London.

Kokelaar, P. and Busby, C. (1992). Subaqueous explosive eruption and welding of pyroclastic deposits. *Science*, 257, 196–201.

Lago, M., Arranz, E., Gil, A., and Pocoví, A. (2004). Magmatismo asociado. In Vera, J. A., editor, *Geología de España*, pages 522–525. Sociedad Geológica de España-Instituto Geológico y Minero de España (SGE-IGME), Madrid.

Lago, M., Arranz, E., Pocovi, A., Martínez, R. M., Gil-Imaz, A., Valenzuela, J. I., and García, J. (1996). Contribución de los magmatismos presentes en la Comunidad Autónoma de Aragón al Patrimonio Geológico. *Geogaceta*, 20(5), 1175–1176.

Lazuen, J. and Roldán, R. (1977). *Mapa Geológico de España 1:50,000 (2nd series), Sheet No. 667 (Villar del Arzobispo)*. IGME, Madrid.

Lee, C.-T. A. and Grand, S. P. (2012). Intraplate volcanism. *Nature*, 482, 314–315.

Manatschal, G., Chenin, P., Ghienne, J.-F., Ribes, C., and Masini, E. (2021). The syn-rift tectono-stratigraphic record of rifted margins (Part I): insights from the Alpine Tethys. *Basin Res.*, 34(1), 457–488.

Martínez, R. M., Lago, M., Valenzuela, J. I., Vaquer, R., and Salas, R. (1996a). El magmatismo alcalino jurásico del sector SE de la Cadena Ibérica: composición y estructura. *Geogaceta*, 20(7), 1687–1690.

Martínez, R. M., Lago, M., Valenzuela, J. I., Vaquer, R., Salas, R., and Dumitrescu, R. (1997a). El volcanismo Triásico y Jurásico del sector SE de la Cadena Ibérica y su relación con los estadios de rift mesozoicos. *Boletín Geológico Min.*, 108 (4, 5)(367–376), 39–48.

Martínez, R. M., Lago, M., Vaquer, R., Arranz, E., and Valenzuela, J. I. (1996b). Precisiones terminológicas entre mecanismos de fragmentación y emplazamiento de rocas volcanoclásticas. *Geogaceta*, 20(3), 515–517.

Martínez, R. M., Lago, M., Vaquer, R., Valenzuela, J. I., and Arranz, E. (1996c). Composición mineral del volcanismo jurásico (pre-Bajociense medio) en la Sierra de Javalambre (Cordillera Ibérica, Teruel): Datos preliminares. *Geogaceta*, 19, 41–44.

Martínez, R. M., Valenzuela, J. I., Lago, M., Bastida, J., and Vaquer, R. (1997b). Origen epiclástico de estratificaciones cruzadas afectando a materiales volcanoclásticos jurásicos en la Sierra de Javalambre (Teruel). *Cuad. Geol. Ibérica*, 22, 121–137.

Martínez, R. M., Valenzuela, J. I., Lago, M., Vaquer, R., and Arranz, E. (1996d). Las rocas volcanoclásticas jurásicas de Albentosa-1 (Cordillera Ibérica, Teruel): Mecanismos de fragmentación y emplazamiento. *Geogaceta*, 19, 45–46.

Martínez, R. M., Vaquer, R., and Lago, M. (1998). El volcanismo jurásico de la Sierra de Javalambre (Cadena Ibérica, Teruel). *Teruel*, 86(1), 43–61.

Martínez-González, R. M., Lago, M., Valenzuela-Ríos, J. I., and Arranz, E. (1996). Interés como Patrimonio Geológico de dos magmatismos mesozoicos en la sierra de Javalambre (Teruel). *Geogaceta*, 20(5), 1186–1188.

McPhie, J., Doyle, M., and Allen, R. (1993). *Volcanic Textures. A Guide to the Interpretation of Textures in Volcanic Rocks*. Centre for Ore Deposit and Exploration Studies (CODES Key Centre), University of Tasmania, Tasmania.

Molina, J. M. and Vera, J. A. (2001). Interaction between sedimentation and submarine volcanism (Jurassic, Subbetic, southern Spain). *Geogaceta*, 29, 142–145.

Molina, J. M. and Vera, J. A. (2008). Resedimented carbonate and volcanic rocks in the Berriasian-Hauterivian of the Subbetic (Alamedilla, Betic Cordillera, southern Spain). *Cretac. Res.*, 29(5–6), 781–789.

Molina, J. M., Vera, J. A., and de Gea, G. (1998). Vulcanismo submarino del Santoniense en el Subbético: Datación con nannofósiles e interpretación (Formación Capas Rojas, Alamedilla, Provincia de Granada). *Estud. Geol.*, 54(5–6), 191–197.

Monaco, P. (1992). Hummocky cross-stratified deposit and turbidites in some sequences of Umbria-Marche area (central Italy) during the Toarcian. *Sediment. Geol.*, 77(1–2), 123–142.

Mutschler, F. E., Larson, E. E., and Gaskill, D. L. (1998). The fate of the Colorado Plateau – A view from the mantle. In Friedman, J. D. and Huffman, A. C., editors, *Laccolith Complexes of Southeastern Utah: Time of Emplacement and Tectonic Setting – Workshop Proceedings*, US Geological Survey Bulletin 2158, pages 203–222. US Geological Survey, Reston, VA.

Nayudu, Y. R. (1971). Geologic implications of microfossils in submarine volcanics. *Bull. Volcanol.*, 35(2), 402–423.

Ortí, F. (1987). La zona de Villel-Cascante-Javalambre. Introducción a las formaciones evaporíticas y al volcanismo jurásico. In Gutiérrez, M. and Meléndez, A., editors, *Libro del XXI Curso de Geología Práctica, Teruel*, pages 53–92. Universidad Verano de Teruel, Teruel.

Ortí, F. and Sanfeliu, T. (1971). *Estudio del vulcanismo jurásico de Caudiel (Castellón) en relación con procesos de lateritización, condensación y silicificación de la serie calcárea*, volume XXVI, pages 21–34. Instituto de Investigaciones Geológicas de la Diputación Provincial, Barcelona.

Ortí, F. and Vaquer, R. (1980). Volcanismo jurásico del sector valenciano de la Cordillera Ibérica. Distribución y trama estructural. *Acta Geol. Hispánica*, 15(5), 127–130.

Osete, M. L., Gómez, J. J., Pavón-Carrasco, F. J., Villalaín, J. J., Palencia-Ortas, A., Ruiz-Martínez, V. C., and Heller, F. (2011). The evolution of Iberia during the Jurassic from palaeomagnetic data. *Tectonophysics*, 502(1–2), 105–120.

Page, K. N. (2003). The Lower Jurassic of Europe: its subdivision and correlation. *Geol. Surv. Denmark Greenland Bull.*, 1, 21–59.

Pavia, G. and Fernández-López, S. (2016). *Pseudoteloceras*, a new stephanoceratid genus (Ammonitida) of the lower Humphriesianum Zone (lower Bajocian, Middle Jurassic) from western Tethys. *Proc. Geol. Assoc.*, 127(2), 196–209.

Pavia, G. and Fernández-López, S. R. (2019). Bajocian Lissoceratinae (Haploceratoidea, Ammonitida) from the Mediterranean-Caucasian Subrealm. *Riv. Ital. Paleontol. Stratigr.*, 125(1), 29–75.

Pellenard, P. and Deconinck, J.-F. (2006). Mineralogical variability of Callovo-Oxfordian clays from the Paris Basin and the Subalpine Basin. *C. R. Geosci.*, 338(12–13), 854–866.

Pellenard, P., Deconinck, J.-F., Huff, W. D., Thierry, J., Marchand, D., Fortwengler, D., and Trouiller, A. (2003). Characterization and correlation of Upper Jurassic (Oxfordian) bentonite deposits in the Paris Basin and the Subalpine Basin, France. *Sedimentologie*, 50(6), 1035–1060.

Pellenard, P., Deconinck, J.-F., Marchand, D., Thierry, J., Fortwengler, D., and Vigneron, G. (1999). Contrôle géodynamique de la sédimentation argileuse du Callovien–Oxfordien moyen dans l'Est du bassin de Paris: influence eustatique et volcanique. *C. R. Acad. Sci. - Ser. IIA - Sciences de la terre et del planètes*, 328(12), 807–813.

Perfit, M. R. and Davidson, J. P. (2000). Plate tectonics and volcanism. In Sigurdsson, H., editor, *Encyclopedia of Volcanoes*, pages 89–113. Academic Press, Cambridge.

Poulaki, E. M. and Stockli, D. F. (2022). The paleotectonic evolution of the western Mediterranean: provenance insights from the internal Betics, Southern Spain. *Front. Earth Sci.*, 10, article no. 9295022.

Puga, E., Fanning, M., Díaz de Federico, A., Nieto, J. M., Beccaluva, L., Bianchini, G., and Díaz Puga, M. A. (2011). Petrology, geochemistry and U–Pb geochronology of the Betic Ophiolites: Inferences for Pangaea break-up and birth of the westernmost Tethys Ocean. *Lithos*, 124(3–4), 255–272.

Puga, E., Morata, D., and Díaz de Federico, A. (2004). Magmatismo mesozoico y metamorfismo de muy bajo grado. In Vera, J. A., editor, *Geología de España*, pages 386–387. Sociedad Geológica de España-Instituto Geológico y Minero de España (SGE-IGME), Madrid.

Quesada, C. and Oliveira, J. T. (2019). Preface. In Quesada, C. and Oliveira, J. T., editors, *The Geology of Iberia: A Geodynamic Approach. The Alpine Cycle*, volume 3, pages xvii–xix. Springer, Berlin.

Salas, R. and Casas, A. (1993). Mesozoic extensional tectonics, stratigraphy and crustal evolution during the Alpine cycle of the eastern Iberian basin. *Tectonophysics*, 228(1–2), 33–55.

Salas, R., Guimerà, J., Mas, R., Martín-Closas, C., Meléndez, A., and Alonso, A. (2001). Evolution of the Mesozoic central Iberian Rift System and its Cainozoic inversion (Iberian chain). In Ziegler, P. A., Cavazza, W., Robertson, A. H. F., and Crasquin-Soleau, S., editors, *Peri-Tethys Memoir 6: Peri-Tethyan Rift/Wrench Basins and Passive Margins*, Mémoires du Muséum National d'Histoire Naturelle 186, pages 145–186. Muséum National d'Histoire Naturelle, Paris.

Sami, T. and Desrochers, A. (1992). Episodic sedimentation on an early Silurian storm-dominated carbonate ramp, Becsie and Merrimack formations, Anticosti Island, Canada. *Sedimentology*, 39(3), 355–381.

Sánchez-Moya, Y. and Sopeña, A. (2004). El rift mesozoico ibérico. In Vera, J. A., editor, *Geología de España*, pages 484–485. Sociedad Geológica de

España-Instituto Geológico y Minero de España (SGE-IGME), Madrid.

Schettino, A. and Turco, E. (2011). Tectonic history of the western Tethys since the Late Triassic. *Geol. Soc. Am. Bull.*, 123(1–2), 89–105.

Sohn, C. and Sohn, Y. K. (2019). Distinguishing between primary and secondary volcaniclastic deposits. *Sci. Rep.*, 9, article no. 12425.

Sohn, R. A. and Sims, K. W. W. (2005). Bending as a mechanism for triggering off-axis volcanism on the East Pacific Rise. *Geology*, 33(2), 93–96.

Sorrentino, L., Stilwell, J. D., and Mays, C. (2014). A model of tephra dispersal from an early Palaeogene shallow submarine Surtseyan-style eruption(s), the Red Bluff Tuff Formation, Chatham Island, New Zealand. *Sediment. Geol.*, 300, 86–102.

Toomey, D. R. (2012). Piecing together rifts. *Nat. Geosci.*, 5(4), 235–236.

Torrens, H. S. (2002). Some personal thoughts on stratigraphic precision in the twentieth century. In Oldroyd, D. R., editor, *The Earth Inside and Out: Some Major Contributions to Geology in the Twentieth Century*, Geological Society London Special Publications 192, pages 251–272. Geological Society of London.

Turner, S., Beier, C., Niu, Y., and Cook, C. (2011). U-Th-Ra desequilibria and the extent of off-axis volcanism across the East Pacific Rise at 9°30'N, 10°30'N, and 11°20'N. *Geochem. Geophys. Geosyst.*, 12(7), article no. Q0AC12.

Valenzuela, J. I., Martínez, R. M., and Lago, M. (1996). Nota preliminar sobre la edad del paleovolcanismo jurásico de Javalambre (Cordillera Ibérica, Teruel). *Geogaceta*, 19, 39–40.

Van Wees, J. D., Arche, A., Beijdorff, C. G., López-Gómez, J., and Cloetingh, S. A. P. L. (1998). Temporal and spatial variations in tectonic subsidence in the Iberian Basin (eastern Spain): inferences from automated forward modelling in high-resolution stratigraphy (Permian-Mesozoic). *Tectonophysics*, 300(1–4), 285–310.

Vera, J. A. (1988). Evolución de los sistemas de depósito en el margen ibérico de la Cordillera Bética. *Rev. Soc. Geol. España*, 1(3–4), 373–391.

Vera, J. A. (2001). Evolution of the South Iberian Continental Margin. In Ziegler, P. A., Cavazza, W., Robertson, A. H. F., and Crasquin-Soleau, S., editors, *Peri-Tethys Memoir 6: Peri-Tethyan Rift/Wrench Basins and Passive Margins*, Mémoires du Muséum National d'Histoire Naturelle 186, pages 109–143. Muséum National d'Histoire Naturelle, Paris.

Vera, J. A., Arias, C., García-Hernández, M., López-Garrido, A. C., Martín-Algarra, A., Martín-Chivelet, A., Molina, J. M., Rivas, P., Ruiz-Ortiz, P. A., Sanz de Galdeano, C., and Vilas, L. (2004). Las Zonas Externas Béticas y el Paleomargen Sudibérico. In Vera, J. A., editor, *Geología de España*, pages 354–361. Sociedad Geológica de España-Instituto Geológico y Minero de España (SGE-IGME), Madrid.

Vergés, J., Kullberg, J. C., Casas-Sainz, A., de Vicente, G., Duarte, L. V., Fernàndez, M., Gómez, J. J., Gómez-Pugnaire, M. T., Jabaloy Sánchez, A., López-Gómez, J., Macchiavelli, C., Martín-Algarra, A., Martín-Chivelet, J., Antón Muñoz, J., Quesada, C., Terrinha, P., Torné, M., and Vegas, R. (2019). An introduction to the Alpine Cycle in Iberia. In Quesada, C. and Oliveira, J. T., editors, *The Geology of Iberia: A Geodynamic Approach. Volume 3: The Alpine Cycle*, pages 1–14. Springer Nature, Heidelberg.

Waitt, R. B. (2007). Primary volcaniclastic rocks: comment and reply: comment. *Geology*, 35, article no. e141.

White, J. D. L. and Houghton, B. F. (2006). Primary volcaniclastic rocks. *Geology*, 34(8), 677–680.

White, J. D. L., Smellie, J. L., and Clague, D. A. (2003). Introduction: a deductive outline and tropical overview of subaqueous explosive volcanism. In White, J. D. L., Smellie, J. L., and Clague, D. A., editors, *Explosive Subaqueous Volcanism*, Geophysical Monograph Series 140, pages 1–23. American Geophysical Union, Washington.

Yang, H., Chemia, Z., Artemieva, I. M., and Thybo, H. (2018). Control on off-rift magmatism: a case study of the Baikal rift zone. *Earth Planet. Sci. Lett.*, 482, 501–509.